

Crystal-structure refinements for orthorhombic boracite, $Mg_3ClB_7O_{13}$, and a trigonal, iron-rich analogue*

By ERIC DOWTY** and JOAN R. CLARK

U. S. Geological Survey, Washington, D.C.

(Received 13 October 1972)

Auszug

Die Kristallstrukturen des rhombischen Boracits, $Mg_3B_7O_{13}Cl$, und seines eisenreichen trigonalen Analogons $Fe_{2.4}Mg_{0.6}B_7O_{13}Cl$ wurden auf Grund von 1509 Interferenzen für den ersten ($Pca\bar{2}1$, $a = b = c/\sqrt{2} = 8,5496 \text{ \AA}$, $c = 12,0910 \pm 0,0009 \text{ \AA}$, $Z = 4$) und 650 Interferenzen für das zweite ($R3c$, $a = 8,612 \pm 0,002 \text{ \AA}$, $c = 21,065 \pm 0,004 \text{ \AA}$, $Z = 6$) bis zu $R = 0,038$ bzw. $0,065$ verfeinert. Die zwei Strukturen sind sehr ähnlich; sie unterscheiden sich nur in der Anordnung der symmetrisch-äquivalenten Einheiten. Sie haben ein zusammenhängendes B-O-Gerüst mit großen Zwischenräumen, in denen sich die Kationen und das Cl-Atom befinden. Das Gerüstmuster besteht aus drei Ringen, die drei B-O-Tetraedern angehören, welche sich in einem gemeinsamen O-Atom, O(1) berühren. Die Ringsysteme sind direkt oder über ein einzelnes B-O-Dreieck miteinander räumlich verknüpft. Das Atom O(1) ist nicht, wie früher beschrieben, vier „ BO_3O -Pyramiden“ gemeinsam, sondern drei dieser „Pyramiden“ sind normale Tetraeder und das vierte ein Dreieck. Die Mg- und Fe-Atome sind fünffach-koordiniert; das sie umgebende Polyeder lässt sich am besten als ein Übergang zwischen tetragonaler Pyramide und trigonaler Bipyramide beschreiben. Die ungewöhnliche Koordination und einige anomale Kation-Chlor-Abstände sind wahrscheinlich durch die Art der Hohlräume bedingt. Bei den meisten Verbindungen mit boracitähnlicher Struktur und mit verschiedenen Kationen und Halogenen als Ersatz für Mg und Cl wurde ein Ansteigen der ferroelektrischen Umwandlungstemperatur mit wachsendem Verhältnis des Ionenradius von Mg^{+2} gegenüber dem des Halogens gefunden.

Abstract

The crystal structures of orthorhombic boracite, $Mg_3ClB_7O_{13}$, and of a trigonal iron-rich analogue, $Fe_{2.4}Mg_{0.6}ClB_7O_{13}$, have been refined using 1509

* Dedicated to Professor M. J. Buerger on the occasion of his 70th birthday.
Publication authorized by the Director, U. S. Geological Survey, Washington, D.C. 20242.

** Present address: Department of Geology and Institute of Meteoritics, University of New Mexico, Albuquerque, New Mexico 87106.

reflections for boracite ($Pca2_1$, $a = b = c/\sqrt{2} = 8.5496 \text{ \AA}$, $c = 12.0910 \pm 0.0009 \text{ \AA}$, $Z = 4$) and 650 reflections for the analogue ($R3c$, $a = 8.612 \pm 0.002 \text{ \AA}$, $c = 21.065 \pm 0.004 \text{ \AA}$, $Z = 6$). The residuals R are, respectively, 0.038 and 0.065. The two structures are quite similar, differing only in the arrangement of symmetry-equivalent units. They consist of unbroken boron-oxygen frameworks with large interstices in which the metal cations and chloride anions reside. The basic unit of the borate framework is made up of three rings of three boron-oxygen tetrahedra sharing corners and joined at a common oxygen atom, O(1); the ring systems are cross-linked to one another, as well as through a single boron-oxygen triangle. The O(1) oxygen atom is not common to four "BO₃O pyramids", as previously described. Instead one of these four is a normal triangle and the other three are normal tetrahedra. Magnesium and iron cations are five coordinated in an arrangement best described as transitional between square pyramidal and trigonal bipyramidal. The nature of the cavities in the borate framework probably accounts for the unusual coordination and some anomalous cation-chlorine distances. For most compounds with boracite-like structures, in which various cations substitute for magnesium and various halogens for chlorine, the ferroelectric transition temperature is found to increase with the ionic radius ratio, Me²⁺/halogen.

Introduction

The interesting "ferro" effects in boracite structures have recently been discussed by a number of authors; for example, the ferroelectric properties by SCHMID (1965, 1970), SCHMID and TROOSTER (1967), KOBAYASHI *et al.* (1968), and ZIMMERMAN *et al.* (1970), to name just a few; the ferromagnetic properties by ASCHER *et al.* (1966); and the ferroelastic properties by AIZU (1968) and TORRE *et al.* (1972). In addition, some optical properties have been discussed by DORMANN (1970), and thermodynamic properties by DVORAK (1971). We cannot hope to mention here all the vast literature which has come out on the boracite-like structures in the past few years.

The structures of boracite and its many synthetic analogues have been assumed to be essentially as described in 1951 by ITO, MORIMOTO, and SADANAGA for the cubic and orthorhombic forms of boracite, Mg₃ClB₇O₁₃. The observed ferroelectric effects have been attributed entirely to movements of metal and halogen atoms, and the borate framework has been assumed "not responsible for the ferroelectricity" (ZIMMERMAN *et al.*, 1970). However, certain features of the accepted structure appeared to be anomalous. The cubic structure, and the orthorhombic one as well, were originally described by Ito *et al.* (1951) as having "BO₃O pyramids", four such pyramids being linked through a common oxygen atom. Such coordination has not been encountered in any of the numerous borate structures studied since 1951, nor is it

compatible with the nuclear magnetic resonance spectra (BRAY *et al.*, 1961; KRIZ and BRAY, 1971). We therefore decided to re-examine the orthorhombic structure. Our results confirm the general features of the orthorhombic structure proposed by ITO *et al.* (1951) but important revisions of the boron-oxygen relationships reveal that there are no "pyramids" in the structure. We have also refined the structure of the trigonal iron-rich analogue¹, $\text{Fe}_{2.4}\text{Mg}_{0.6}\text{ClB}_7\text{O}_{13}$, and have found that the borate framework is essentially the same. A preliminary report on the borate framework has appeared (DOWTY and CLARK, 1972a), and a note concerned with the ferroelectric and ferroelastic aspects has been published (DOWTY and CLARK, 1972b). Prof. J. J. PAPIKE and Dr. SHIGEHO SUENO, State University of New York at Stony Brook, are collecting data above the orthorhombic-cubic transition temperature on the same boracite crystal used during this study, and their results will be published elsewhere.

Experimental work

Crystallographic and chemical data

The large (some greater than 0.5 cm diameter) crystals showing cubic morphology, in which boracite and its iron analogue are often found, are intensely twinned on a microscopic scale. To obtain material suitable for diffraction studies, it was necessary to crush these large pseudomorphs and select small untwinned fragments. The crystal of boracite selected for study was an irregular fragment with trapezoidal shape from a specimen originating at Solvayshall, Roschwitz, Germany (U. S. National Museum No. B12325); the size of the fragment was $0.23 \times 0.16 \times 0.10$ mm. It was verified optically to be a single domain. The optical orientation is given in Table 1, together with the cell constants obtained from measurements of standard powder diffractometer data refined by least-squares methods (APPLEMAN *et al.*, in press). No chemical analysis was made during this study; the boracite is assumed to be almost pure.

The crystal of the iron-rich analogue originated at Bischofferode, Thüringen, Germany, and it was also an irregular fragment, 0.13×0.10

¹ The crystal was chosen from a sample labelled "ericaite" (HEIDE, 1955; KÜHN and SCHAAKE, 1955) and was thus designated in early notes (DOWTY and CLARK, 1972a,b). However, the nomenclature is uncertain following the recent description of "congolite" (WENDLING *et al.*, 1972). We therefore refer here to the "trigonal iron-rich analogue of boracite" rather than using either mineral name.

Table 1. Crystallographic data for boracite and the iron-rich analogue

Symmetry Space group	Boracite Orthorhombic <i>Pca2</i> ₁	Iron-rich analogue* Trigonal <i>R3c</i>
Cell constants		
<i>a</i>	$c/\sqrt{2} = 8.5496$	$8.612 \pm 0.002 \text{ \AA}$
<i>b</i>	$c/\sqrt{2} = 8.5496$	$8.612 \pm 0.002 \text{ \AA}$
<i>c</i>	12.0910 ± 0.0009	$21.065 \pm 0.004 \text{ \AA}$
Cell volume	883.81	1353.0 \AA^3
<i>Z</i>	4 [Mg ₃ ClB ₇ O ₁₃]	6 [Fe _{2.4} Mg _{0.6} ClB ₇ O ₁₃]
Calc. density	2.945	3.443 g/cm ³
Optical orientation	<i>X</i> = <i>c</i> , <i>Y</i> = <i>a</i> , <i>Z</i> = <i>b</i>	

* Corrected from values given by DOWTY and CLARK (1972b).

$\times 0.07$ mm. Optical examination showed that this crystal contained from five to ten percent of a second domain with a different orientation. As no better crystal could be found, we assumed that the slight admixture would not cause major problems. Indeed the results do not seem to be those that would be expected for a superposition of structures due to undetected domains. Cell constants for this material, obtained as were those for boracite, are given in Table 1. From the previously published analysis (KÜHN and SCHAAKE, 1955), the crystal is assumed to have about twenty percent of the iron replaced by magnesium, so its formula is taken as Fe_{2.4}Mg_{0.6}ClB₇O₁₃. Careful examination of single-crystal precession photographs and monitoring of equivalent reflections during data collection revealed no departure from *R3c* symmetry.

Single-crystal x-ray diffraction data

Data for both crystals were collected on a Picker single-crystal automatic diffractometer by 2θ -scan methods, using Nb-filtered Mo x-radiation and a scintillation-counter detector. The scan range was calculated as suggested by ALEXANDER and SMITH (1964). Background counts of 20 seconds duration were made for each reflection at the beginning and end of the scan range. The boracite crystal was mounted with *b* parallel to the φ axis and 2621 reflections were measured. The iron-rich analogue was mounted with *c* parallel to the φ axis and 1591

reflections were measured. In each case a standard reflection was monitored after every 30 measurements.

Computer programs written by Prof. C. T. PREWITT, State University of New York at Stony Brook, and modified for the IBM 360/65 by D. E. APPLEMAN, U. S. Geological Survey, were used to obtain the diffractometer settings and to reduce the raw data, including corrections for the total background count and for Lorentz and polarization factors. No absorption corrections were made for boracite ($\mu = 7.6 \text{ cm}^{-1}$), or for the iron-rich analogue ($\mu = 43.6 \text{ cm}^{-1}$). The observed $|F_o|$ was less than four times its standard deviation from background as determined by the counting statistics for 1112 reflections of boracite and 841 reflections of the iron-rich analogue; these reflections were coded as "less-thans" and omitted during the refinements, which used 1509 reflections for boracite and 650 reflections for the trigonal analogue.

Refinement procedures

The computer program ORFLS (Busing *et al.*, 1962) was used for preliminary refinement of boracite. Programs RFINE and BADTEA, written by Dr. L. W. FINGER, Geophysical Laboratory, Washington, D. C., were used for the final refinement of boracite and all refinement of the iron-rich form, as well as for calculation of bond distances, bond angles, and thermal ellipsoids. The scattering factors were calculated from a nine-coefficient analytical function (CROMER and WABER, 1965) using the coefficients given by CROMER and MANN (1968) for neutral atoms.

The atomic parameters given by ITO *et al.* (1951) were used initially for the orthorhombic boracite; four cycles of least-squares refinement for positional parameters and individual isotropic temperature factors reduced the conventional $R = \sum |F_o| - |F_c| / \sum |F_o|$ from 0.275 to 0.061, and nine more cycles refining anisotropic temperature parameters reduced R to 0.038. Six intense reflections presumed to be affected by extinction were removed after the sixth cycle. A three-dimensional electron-density Fourier synthesis and the associated difference Fourier synthesis were then calculated using the *X-Ray 67, Program system for x-ray crystallography* by J. M. STEWART, University of Maryland (adapted for the IBM 360/65 by D. E. APPLEMAN, U. S. Geological Survey). No unusual features were noted and the maximum difference observed was $\pm 0.7 \text{ e}/\text{\AA}^3$.

The locations of the (Fe,Mg) and Cl atoms in the iron-rich analogue were assumed to be as proposed by SCHMID (1970), but the locations

of the boron and oxygen atoms were derived by analogy with our previously refined structure of boracite. A total of nine cycles of refinement, the later ones with anisotropic temperature factors, reduced R to 0.065. The Fourier difference map showed features sometimes

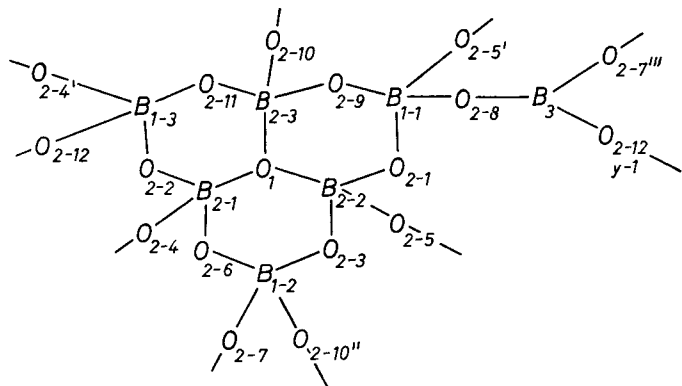


Fig. 1. Schematic diagram of the asymmetric unit that forms the borate framework in boracite and its analogue, numbered as for the orthorhombic structure (Table 2)

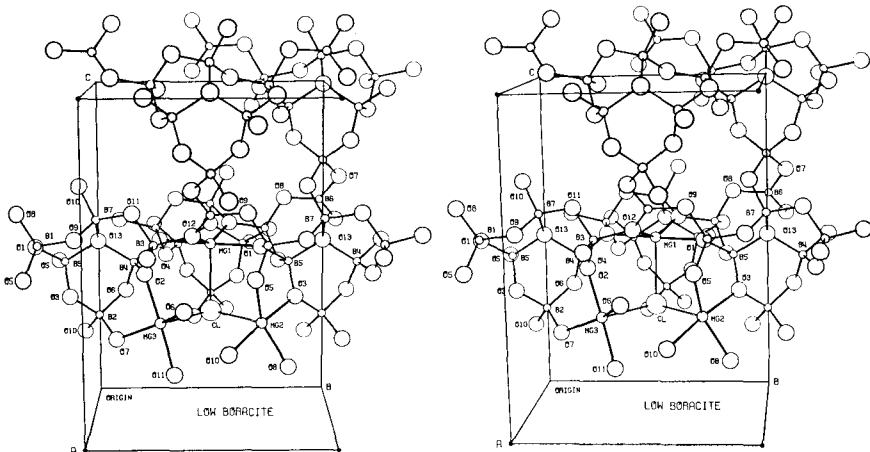


Fig. 2. Stereoscopic-pair view of selected portions of the borate framework in orthorhombic boracite. Atom labelling as follows: O(13) = O(1), others are O(2) atoms; B(1), B(2), B(3) are the B(1) set, B(4), B(5), B(7) are the B(2) set; B(6) = B(3). The close approach of B(3) to O(1) can be seen at mid-right between labelled B(6) and O(13). Drawing produced by ORTEP (JOHNSON, 1965)

Table 2. *Atomic and thermal parameters for orthorhombic*

Crystal	Atom	<i>x</i>	<i>y</i>	<i>z</i>	Equivalent isotropic <i>B</i>
O	Cl	0.0241 (1)	0.4994 (2)	0.2618	0.92 Å ²
T	Cl	0.0	0.0	0.2654 (2)	1.16
O	Mg(1)	-0.0083 (2)	0.4988 (3)	0.4770 (2)	0.59
T	(Fe,Mg)	0.1480 (4)	0.2971 (2)	0.3270	0.74
O	Mg(2)	0.2351 (2)	0.7204 (2)	0.2537 (2)	0.62
O	Mg(3)	0.2350 (2)	0.2784 (2)	0.2514 (2)	0.59
O	B(1)-1	0.2482 (7)	0.7483 (6)	0.5018 (5)	0.26
T	B(1)-1	0.162 (3)	-0.169 (3)	0.0828 (5)	0.59
O	B(1)-2	0.0060 (5)	0.9987 (9)	0.2488 (5)	0.43
O	B(1)-3	0.2481 (7)	1.2523 (7)	0.5016 (6)	0.46
O	B(2)-1	0.0023 (5)	1.1537 (7)	0.4202 (6)	0.46
T	B(2)	0.099 (2)	-0.105 (2)	-0.0286 (4)	0.78
O	B(2)-2	0.0035 (5)	0.8464 (7)	0.4224 (6)	0.50
O	B(2)-3	0.1553 (4)	0.9999 (6)	0.5735 (4)	0.50
O	B(3)	0.2972 (5)	0.5000 (7)	0.6012 (4)	0.51
T	B(3)	0.0	0.0	0.102 (1)	0.96
O	O(1)	0.0173 (3)	0.9993 (5)	0.4914 (3)	0.40
T	O(1)	0.0	0.0	-0.0126 (6)	0.70
O	O(2)-1	0.0824 (3)	0.7218 (4)	0.4794 (4)	0.34
T	O(2)-1	-0.160 (1)	-0.001 (1)	0.1056 (3)	0.59
O	O(2)-2	0.1606 (4)	1.2107 (4)	0.4019 (4)	0.39
T	O(2)-2	0.289 (1)	0.261 (1)	-0.0353 (3)	0.64
O	O(2)-3	0.0789 (3)	0.8753 (4)	0.3156 (4)	0.41
T	O(2)-3	0.199 (1)	-0.022 (1)	-0.0869 (3)	0.67
O	O(2)-4	-0.0857 (4)	1.2701 (4)	0.4813 (4)	0.41
T	O(2)-4	-0.306 (1)	-0.226 (1)	0.0204 (3)	0.66
O	O(2)-5	-0.1604 (4)	0.8072 (4)	0.4059 (4)	0.44
O	O(2)-6	-0.0730 (4)	1.1153 (4)	0.3172 (4)	0.50
O	O(2)-7	0.1330 (3)	1.0801 (4)	0.1865 (3)	0.38
O	O(2)-8	0.2885 (4)	0.6613 (3)	0.6066 (4)	0.52
O	O(2)-9	0.2837 (4)	0.9129 (4)	0.5226 (4)	0.29
O	O(2)-10	0.1109 (3)	0.9243 (4)	0.6764 (3)	0.33
O	O(2)-11	0.2004 (4)	1.1597 (3)	0.5965 (3)	0.35
O	O(2)-12	0.2075 (4)	0.4206 (4)	0.5261 (4)	0.45

greater than $\pm 1.0 \text{ e/Å}^3$ at locations distinct from the final atomic positions. The locations of these features, however, could be rationalized on the basis of a "ghost" structure due to the presence of the second minor domain in a twin relationship.

The atomic parameters obtained are listed in Table 2 for both crystals, and the structure factors calculated with these parameters are

boracite (*O*) and an iron-rich, trigonal analogue (*T*)

Parameter*	β_{22}	β_{33}	β_{12}	β_{13}	β_{23}
β_{11}					
35 (1)	28 (1)	16 (1)	0.6 (1.4)	0.8 (7)	-0.6 (1.0)
50 (3)	50	7 (1)	25	0	0
15 (1)	13 (1)	16 (1)	-0.5 (1.0)	0.6 (1.3)	-2 (2)
34 (3)	38 (2)	3.8 (1)	19 (3)	1 (1)	3 (1)
23 (2)	21 (2)	10 (2)	9 (1)	0.3 (1.4)	-2 (1)
24 (2)	21 (2)	8 (2)	-9 (2)	2 (1)	-1 (1)
12 (5)	7 (5)	4 (4)	4 (4)	-4 (2)	-3 (2)
24 (18)	57 (23)	2 (2)	32 (13)	-3 (7)	-4 (7)
12 (3)	12 (3)	10 (4)	-3 (4)	-4 (3)	3 (5)
17 (6)	13 (6)	11 (5)	0 (5)	1 (3)	2 (3)
11 (5)	7 (5)	15 (5)	2 (3)	1 (3)	7 (4)
11 (17)	43 (21)	2 (1)	6 (9)	-6 (6)	-9 (7)
22 (5)	13 (5)	0 (4)	0 (3)	-3 (3)	5 (4)
14 (3)	13 (3)	2 (3)	7 (4)	1 (2)	-5 (3)
21 (3)	12 (3)	10 (4)	1 (5)	-5 (2)	1 (4)
28 (9)	28	9 (3)	14	0	0
15 (3)	8 (2)	9 (3)	4 (3)	-3 (2)	-2 (3)
23 (8)	23	6 (2)	11	0	0
7 (3)	13 (3)	7 (2)	-2 (2)	-2 (2)	-2 (2)
18 (8)	24 (9)	4 (1)	9 (7)	-2 (3)	-2 (3)
15 (3)	18 (3)	4 (3)	-3 (2)	3 (2)	2 (2)
24 (9)	35 (10)	3 (1)	14 (8)	-1 (3)	-3 (3)
13 (3)	14 (3)	8 (3)	2 (2)	0 (2)	2 (2)
25 (9)	30 (9)	1 (1)	-5 (8)	-1 (3)	-1 (2)
13 (3)	11 (3)	9 (3)	-1 (2)	-1 (2)	-3 (2)
49 (11)	12 (8)	3 (1)	11 (8)	1 (3)	3 (2)
8 (3)	13 (3)	12 (3)	-4 (2)	0 (2)	1 (2)
17 (3)	15 (3)	10 (3)	5 (2)	-2 (2)	-2 (2)
18 (3)	14 (3)	4 (3)	-5 (2)	3 (2)	-3 (2)
19 (3)	6 (3)	14 (3)	3 (2)	0 (2)	2 (2)
17 (3)	8 (3)	2 (3)	-1 (2)	1 (2)	-3 (2)
16 (3)	10 (3)	4 (3)	4 (2)	0 (2)	1 (2)
16 (3)	11 (3)	5 (3)	-1 (2)	-1 (2)	0 (2)
17 (3)	10 (3)	9 (3)	0 (2)	-4 (2)	-1 (2)

* Error in parentheses is one standard deviation; for 0.0241 (1) read 0.0241 ± 0.0001 , etc. β_{ij} are given times 10^4 . Temperature factor form $\exp \left\{ - \sum_{i=1}^3 \sum_{j=1}^3 h_i h_j \beta_{ij} \right\}$.

compared with the observed in Table 3. The thermal ellipsoid data are presented in Table 4 for boracite only.

Table 3. Comparison of observed and calculated structure factors.
A. Boracite. * indicates "less-than" reflections

h	k	l	F_o	F_c	h	k	l	F_o	F_c	h	k	l	F_o	F_c	h	k	l	F_o	F_c	
1	0	0	0.3*	0.0	13	6	0	0.9*	4.4	3	14	0	7.8	7.5	5	7	1	26.7	26.1	
2		18.2	14.2	14	14.5	14.7	4			23.2	22.2	7	44.9	44.5	12			8.6	8.9	
3		0.4*	0.0	14	7	0	0.9*	3.5	5	0.9*	0.6	8	5.2*	3.1	11			0.8*	0.0	
4		117.8	130.8	13	27.2	26.9	6			24.8	24.6	9	15.2	14.9	10			48.7	48.1	
5		0.7*	0.0	12		0.9*	2.2	7		1.0*	2.4	10	19.3	18.7	9			1.5*	0.0	
6		6.1	4.0	11		0.8*	0.9	8		19.5	19.3	11	10.5	10.5	8			5.6	7.7	
7		2.7*	0.0	10		8.1	6.2	9		5.2*	4.5	12	7.3	5.4	7			0.6*	0.0	
8		55.5	55.9	9	26.2	27.8	9	14	1	13.1	12.8	13	9.2	8.9	6			54.8	54.6	
9		2.7*	0.0	8		0.7*	0.9	8		1.0*	6.0	14	3.9	9.7	5			0.5*	0.0	
10		25.5	26.2	7	74.0	75.3	5			8.0	0.2	16	6	1	0.9*	1.4	14	10.4	10.4	
11		0.8*	0.0	6		0.7*	1.2	6		16.2	16.9	13	8.3	0.4	3			0.4*	0.0	
12		39.5	38.7	5	22.7	23.7	5			10.5	10.2	12	25.4	25.1	2			37.0	37.0	
13		0.9*	0.0	4	8.5	8.4	4			0.9*	0.7	11	21.8	21.5	1			0.3*	0.0	
14	1	0	0.9*	0.1	3	33.2	33.1	2			14.2	15.7	10	11.4	12.2	0			0.3*	0.0
15		4.6*	6.1	2	0.6*	0.6	1			0.9*	1.4	9	13.3	13.1	0	0	2	48.1	54.1	
12		0.3*	2.5	1	0.6*	1.8	0			0.9*	0.6	8	12.2	13.6	1			0.4*	0.0	
11		7.5	9.1	0	13.9	11.9	0	13	1	0.9*	0.0	7	1.7*	0.8	3			0.4*	0.0	
10		0.7*	1.0	8	73.5	74.2	1			7.0*	8.9	6	22.4	21.3	4			2.0*	3.6	
9		17.2	16.8	2	10.1	1.2	2			0.9*	5.5	5	0.6*	1.4	5			0.5*	0.0	
8		2.7*	3.4	2	64.1	64.9	3			11.1	12.2	4	33.2	32.9	6			49.7	49.0	
7		0.6*	1.7	3	4.5*	7	4			6.7*	3.0	3	7.2	38.9	7			0.6*	0.0	
6		13.8	15.7	4	66.1	66.9	5			17.4	12.0	2	0.6*	6.6	21.1			0.5*	0.0	
5		58.1	58.9	5	0.7*	2.3	6			10.3	11.0	1	39.3	39.3	9			0.7*	0.0	
4		7.3	6.1	6	4.7*	4.6	7			5.1*	8.8	0	6.7	0.0	10			35.3	35.7	
3		74.3	75.6	7	0.7*	1.1	8			13.1	13.9	0	5	1	0.5*	0.0	11	0.7*	0.0	
2		1.9*	0.6	8	25.1	24.1	9			10.9	15.0	1	48.7	48.7	12			49.4	48.6	
1		47.0	50.6	9	0.8*	1.1	10			1.0*	2.5	2	16.4	44.2	15			0.9*	0.0	
0		0.3*	0.5	10	5.9*	6.2	11	12	1	1.0*	0.4	3	29.8	29.0	14			19.1	18.7	
0	2	0	5.7	0.9	11	9.2	8.8	10			8.3	9.9	4	4.0*	4.3	14	1	2	1.5*	4.1
1		5.4*	2.4	12	31.9	31.4	9			15.0	12.9	5	36.1	35.7	15			17.1	17.9	
3		3.4*	1.7	13	12.7	13.5	8			19.4	20.1	6	0.6*	2.3	12			0.8*	0.8	
4		29.0*	27.9	14	0.7*	3.2	7			8.7	8.0	7	17.8	17.5	11			12.9	14.1	
5		2.9*	3.2	15	9	1.0*	3.6	6		7.6	8	8	17	14.8	10			6.9	7.5	
6		108.4	111.2	13	3.2*	3.4	5			11.1	10.6	9	10.3	38.7	9			22.2	22.9	
7		2.3*	3.4	12	0.9*	3.9	4			7.7	10.4	10	5.8	3.6	8			3.0*	3.8	
8		15.4	15.6	11	0.9*	3.1	3			11.1	12.3	11	1.0*	4.5	7			20.4	19.0	
9		5.7	5.9	10	5.0*	5.8	2			0.8*	2.2	12	0.8*	4.9	6			4.0*	6.0	
10		45.9	44.3	9	41.8	39.9	1			6.7	5.6	13	14.6	12.7	5			30.8	28.8	
11		4.2*	6.4	8	0.8*	0.5	0			0.8*	0.0	14	3.4*	3.8	4			6.2	5.9	
12		32.5	32.1	7	9.2	8.3	0	11	1	5.5*	0.0	14	14.5	15.7	3			54.7	50.8	
13		0.8*	2.2	6	0.8*	2.4	1			14.6	15.6	13	16.3	12.2	2			0.4*	1.7	
14		9.6	10.9	5	35.9	35.4	2			4.3*	7.4	12	14.6	14.9	1			16.7	14.1	
15	3	0	0.9*	7.8	4	0.7*	1.2	3			31.4	31.1	11	20.1	19.6	0			0.3*	0.8
16		0.4*	1.0	5	21.0	20.9	4			19.8	20.1	10	29.1	29.0	9	2	2	72.9	74.2	
17		4.6*	7.7	4	2.7*	3.2	5			12.5	12.3	9	16.0	16.1	1			0.4*	1.7	
18		21.2	20.3	1	38.8	38.6	6			22.0	22.5	8	9.7	10.2	2			86.4	88.5	
19		6.9	7.0	0	0.8*	5.6	7			22.5	22.1	7	13.3	13.6	5			10.9	10.1	
20		0.7*	0.6	10	56.5	56.8	8			20.5	19.9	6	45.1	44.4	4			91.3	91.3	
8		5.5	4.7	1	2.0*	1.8	9			9.1	11.4	5	5.3	5.3	5			5.6	5.7	
7		32.8	32.1	2	33.8	33.8	10			0.9*	3.8	4	5.2	5.0	6			9.9	8.7	
6		11.0	11.2	3	7.5	8.5	11			1.0*	7.6	3	0.5*	2.7	7			11.2	11.3	
5		58.2	55.9	4	12.9	12.4	12			0.9*	1.4	2	21.6	21.7	8			21.7	20.9	
4		0.5*	1.7	5	3.9*	1.2	13	10	1	0.9*	1.0	1	105.5	104.1	9			5.9	8.5	
5		29.8	33.0	6	37.2	36.8	12			6.4*	9.5	0	0.4*	0.0	10			8.1	9.7	
2		0.4*	0.6	7	0.8*	4.0	11			0.9*	3.1	0	3.1	0.4	0	11		3.6*	4.4	
1		0.9*	9.6	8	0.8*	3.2	10			0.9*	10.1	1	30.3	30.5	12			10.0	12.0	
0		2.6*	4.2	9	3.7*	3.5	9			0.9*	5.6	2	7.2	6.4	15			0.8*	0.7	
0	4	0	117.0	123.0	10	1.0*	3.0	3		8.1	8.8	5	55.3	54.8	14			8.1	8.0	
2		4.5	4.2	11	0.9*	1.5	7			11.9	12.0	4	4.8*	2.7	14	3	2	0.7*	6.0	
3		35.2	35.4	12	0.9*	3.6	6			21.2	19.8	5	7.0	7.5	13			27.4	25.2	
4		0.5*	4.4	13	0.9*	1.7	5			0.8*	2.0	6	45.3	42.2	12			0.8*	1.3	
5		95.2	96.9	5	3.9*	1.2	14			2.9	6.9	7	31.5	30.1	11			12.0	12.1	
6		0.6*	1.2	11	1.0*	3.1	3			22.5	21.5	8	33.3	33.9	10			7.4	8.8	
7		21.3	20.9	10	0.9*	2.1	2			4.2*	7.1	9	23.7	23.0	9			31.2	31.3	
8		3.7*	4.8	9	0.9*	0.6	1			17.2	16.8	10	38.0	17.6	8			0.7*	4.4	
9		5.7*	59.2	8	5.6*	3.0	0			0.7*	0.0	11	14.1	15.7	7			36.2	37.4	
10		3.7*	4.2	7	11.5	11.3	9	9	1	1.9*	0.0	12	6.9	7.4	6			12.5	12.2	
11		10.9	12.1	5	21.9	21.6	2			35.7	34.1	15	12.6	13.6	5			41.8	41.4	
12		35.0	35.7	4	0.8*	1.4	3			18.8	16.6	14	2.8*	6.6	3			34.2	31.8	
13		5.2*	9.0	3	35.7	34.9	4			10.4	10.5	15	9.4	8.2	2			2.6	9.1	
14		19.0	18.0	2	0.8*	3.1	7			0.7*	4.2	4	30.7	29.6	1			72.0	70.2	
15		5.4*	3.7	6	34.3	34.1	14			7.4*	8.0	5	7.2	6.0	7			0.6*	2.9	
5		34.8	33.5	7	12.5	12.9	14	8	1	7.3*	12.0	9	7.2	7.2	8			15.1	16.6	
4		0.6*	2.5	8	28.9	28.4	13			17.9	18.6	1	0.4*	0.0	0			0.7*	4.1	
3		72.7	70.8</td																	

Table 3A. (Continued)

<i>h</i>	<i>k</i>	<i>l</i>	F_o	F_c	<i>h</i>	<i>k</i>	<i>l</i>	F_o	F_c	<i>h</i>	<i>k</i>	<i>l</i>	F_o	F_c	<i>h</i>	<i>k</i>	<i>l</i>	F_o	F_c	
2	5	2	-0.5*	2.8	10	12	2	4.0*	5.1	12	8	3	11.7	9.9	2	2	3	12.7	12.7	
1	47	7	55.5	11	0.9*	2.2	11	0.9*	4.2	1	3	3.5*	3.3	11	4.1*	5.0	11.6	12.6		
0	12	5	12.1	10	13	2	1.0*	3.8	10	15.7	14.6	0	0.4*	0.0	12	33.6	32.2			
0	6	2	16.3	16.2	9	8.6	6.6	9	15.2	16.7	0	1	3	0.4*	0.0	13	0.9*	3.3		
1	4.9	4.0	8	0.9*	2.0	8	19.5	18.6	1	23.6	24.0	14	13.0	12.7						
2	37.2	38.1	7	9.2	9.6	7	15.5	15.5	2	3.6*	2.8	14	5	4	3.2*	3.0				
3	2.9*	6.0	6	0.9*	8.1	6	10.1	11.1	3	4.7	4.0	15	17.6	19.4						
4	6.7	5.1	5	13.9	12.8	5	0.7*	1.1	4	2.2*	4.1	12	0.9*	1.9						
5	3.5*	4.2	4	5.6*	4.3	4	21.0	21.7	5	50.2	51.3	11	0.8*	4.0						
6	25.9	26.3	5	25.9	26.3	5	33.5	33.4	6	25.3	24.6	10	8.4	9.9						
7	0.1	1.5	2	4.4*	5.5	2	5.5	6.3	7	30.6	30.8	9	25.4	24.5						
8	36.5	36.9	5	17.7	18.5	1	51.7	52.3	8	32.7	32.6	8	5.5*	1.2						
9	0.8*	3.2	0	6.0*	5.1	0	3.0*	3.0	9	31.1	31.6	7	4.6*	3.2						
10	0.8*	3.1	0	7.2*	8.8	0	7	3	10	18.6	19.2	6	10.1	10.8						
11	0.8*	2.4	1	0.9*	2.7	1	39.0	38.9	11	28.3	28.5	5	34.3	32.4						
12	11.5	9.8	2	18.2	18.8	2	16.9	18.9	12	7.0	8.5	4	0.6*	1.9						
13	3.0*	1.3	3	0.9*	2.0	3	45.1	45.8	13	10.9	11.6	3	17.9	18.6						
14	8.0	7.1	4	15.7	16.9	4	0.6*	4.9	14	15.9	15.1	2	8.4	7.8						
14	7	2	0.9*	3.2	5	0.9*	5.7	5	12.7	12.4	14	0	3	25.3	25.1	1	57.9	57.5		
15	19.3	19.5	6	16.3	15.2	6	17.7	18.8	15	0.8*	0.0	0	4.5	3.3						
12	0.9*	5.8	7	3.5*	1.8	7	37.9	37.0	12	10.9	12.4	0	6	4	33.7	32.7				
11	7.7	8.4	8	16.2	16.2	8	11.2	12.0	11	0.8*	0.0	1	3.4*	0.5						
10	0.8*	2.7	0	1.0*	0	9	8.8	8.6	10	35.9	35.5	2	120.4	124.5						
9	10.4	10.6	9	14	3	1.0*	7.1	10	9.7*	10.0	5	0.6*	1.1							
2	2.9*	5.4	8	5.5*	1.6	11	35.1	34.4	8	13.6	14	4	40.5	40.0						
7	3.6*	4.7	7	7.5	7.9	12	0.9*	5.6	7	0.6*	0.0	5	6.9	6.6						
6	0.7*	3.3	6	12.0	12.4	13	10.1	12.9	6	39.3	39.6	5	64.3	65.0						
5	39.2	39.5	5	9.4	10.6	14	7.9*	7.8	5	0.5*	0.0	7	0.7*	1.9						
4	6.3	7.2	4	0.9*	6.8	4	11.5	11.3	4	19.2	18.3	8	21.7	21.4						
3	28.8	27.8	3	13.4	12.2	13	4.0*	5.5	3	0.5*	0.0	9	5.0*	4.0						
2	2.2*	3.6	2	0.9*	4.3	12	16.4	15.7	2	44.1	44.0	10	15.2	12.8						
1	35.9	35.8	1	11.7	12.1	11	9.9*	10.2	1	2.4*	0.0	11	0.8*	2.2						
2	7.8	7.4	0	0.9*	0.0	10	0.8*	2.1	0	0.4*	0.0	12	15.8	15.9						
0	8	2	20.7	20.7	0	13	5	0.9*	0.0	9	2.1*	0	4	0.4*	0.0	13	0.9*	0.3		
1	6.8	6.6	1	10.2	18.1	8	40.0	37.7	2	73.1	73.1	14	10.4	9.9						
2	25.7	25.3	2	6.3*	8.6	7	11.9	12.2	3	0.4*	0.0	14	7	4	0.7*	2.1				
3	0.7*	4.2	3	7.0*	8.0	6	5.9*	6.6	5	0.5*	0.0	13	23.9	22.6						
4	8.8	7.7	4	8.5	10.4	5	14.5	15.2	6	63.0	61.7	12	4.6*	1.0						
5	0.7*	1.7	5	21.6	20.1	4	10.4	19.2	7	4.1*	0.0	11	13.2	14.9						
6	17.1	16.8	6	5.7*	5.8	5	0.6*	1.4	8	79.7	79.8	10	0.8*	3.8						
7	2.2*	2.9	7	7.5	8.2	2	14.0	14.0	9	0.7*	0.0	9	0.8*	5.8						
8	22.7	22.0	8	0.9*	2.3	1	23.2	22.3	10	3.6*	4.4	8	0.8*	1.7						
9	7.2	6.9	9	15.8	17.2	0	0.6*	0.0	11	0.8*	0.0	7	32.3	31.9						
10	11.	15.1	10	1.0*	2.4	0	0.5*	0.0	12	32.7	31.2	6	0.7*	6.4						
11	5.4*	8.2	11	2	1.0*	2.3	1	4.0*	2.9	14	0.9*	3.6	5	20.5	19.4					
12	6.2*	9.7	10	0.9*	2.5	2	49.7	50.2	15	1.4*	2.4	4	4.6*	5.5						
13	5.0*	4.9	4	0.9*	4.1	3	31.6	31.9	14	7.4	7.2	4	6.5*	6.6						
14	1.0*	5.4	8	27.3	26.6	4	45.8	45.3	12	12.0	12.5	2	8.2	8.1						
15	12.2	12.4	6	0.9*	1.4	6	15.3	15.1	11	11.0	12.0	0	9.7	10.5						
12	0.9*	3.5	3	13.0	14.2	8	1.6*	2.1	9	30.2	29.6	1	0.7*	2.0						
13	34.5	33.6	4	13.0	14.2	8	30.9	30.0	8	4.8*	7.1	2	39.6	40.2						
10	0.9*	7.1	3	10.8	11.0	9	24.9	24.0	7	24.6	23.8	3	9.5	9.6						
9	0.8*	2.4	1	7.7	8.9	11	27.3	26.8	6	2.6*	3.5	4	54.3	52.8						
8	19.0	18.8	0	0.8*	0.0	12	16.8	19.4	12	63.5	62.2	5	5.0*	5.4						
7	7.5	7.8	0	0.8*	0.0	13	16.8	19.4	4	0.5*	0.5	6	20.6	20.8						
6	7.5	7.8	0	0.8*	0.0	15	16.8	19.4	4	0.5*	0.5	6	6.5	7.6						
5	25.3	24.5	1	21.5	21.0	14	4	25.6	25.9	2	23.1	21.2	7	6.5	7.6					
4	0.7*	4.3	2	21.5	21.0	14	4	25.6	25.9	2	2.1*	3.4	8	50.6	33.6					
3	22.9	23.5	3	25.2	23.2	15	12.6	12.9	1	82.8	82.3	9	4.5*	6.8						
2	0.7*	3.5	4	18.7	18.7	12	0.8*	1.4	0	2.1*	3.1	10	12.5	13.5						
1	7.9	9.6	5	10.0	10.0	11	19.5	21.2	1	46.8	44.8	11	0.9*	2.1						
0	9.2	8.2	6	13.0	12.5	10	36.7	36.4	1	4.7	4.5	12	25.9	25.2						
0	10	2	23.3	22.7	6	22.8	22.7	9	20.3	20.7	2	118.2	127.5	15	0.9*	2.7				
1	4.5*	2.2	8	0.9*	4.9	8	16.4	16.6	3	1.5*	4.4	14	12.6	8.5						
2	7.4	6.0	9	13.4	13.5	7	3.7*	4.3	4	29.6	27.9	13	9	4	24.8	23.8				
3	8.4	8.9	10	10.2	12.4	3	33.4	33.5	5	0.5*	3.5	12	1.8*	5.9						
4	19.7	19.7	11	23.1	24.0	4	48.6	46.7	15	24.3	25.8	1	43.2	42.3						
5	0.8*	4.8	12	4.1*	5.1	4	10.4	7	7	0.9*	1.0	10	0.9*	5.8						
6	14.1	15.5	4	0.9*	1.6	3	45.0	40.9	8	22.4	21.2	9	0.9*	6.5						
7	6.8	8.3	12	0.9*	2.0	2	13.8	13.5	9	6.6	4.7	8	5.2*	5.7						
8	12.9	13.7	11	9.9	7.2	1	5.5	5.0	10	35.4	34.5	7	9.9	8.2						
9	9.9	11.3	10	21.3	20.5	0	0.5*	0.0	11	4.0*	6.4	6	7.4	8.5						
10	8.6	7.1	9	26.6	26.9	0	0.5*	0.0	12	17.3	17.0	5	14.6	14.6						
11	4.7*	3.9	8	20.1	19.4	1	19.4	19.8	13	6.2*	5.9	4	3.2*	5.3						
12	0.9*	2.3	7	0.8*	3.5	2	108.1	108.7	14	15.2	14.									

Table 3A. (Continued)

b	k	l	F _o	F _c	b	k	l	F _o	F _c	b	k	l	F _o	F _c	b	k	l	F _o	F _c	
5	11	4	26.2	25.2	3	9	5	17.9	18.0	14	3	5	15.6	15.7	5	3	6	36.3	36.1	
4		1.1*	1.4	4		0.7*	5.1	14	2	5	0.9*	5.6	4	6.2	6.1	6	0.8*	5.3		
3		7.1	8.6	4		26.2	25.0	13		14.1	13.9	3	32.5	31.3	7	3.1*	6.2			
2		0.8*	4.6	6		26.0	24.4	12		34.9	34.4	2	0.5*	1.8	8	7.9	9.0			
1		13.4	14.1	7		7.9	9.1	11		5.4*	6.9	1	54.5	54.2	9	0.9*	5.1			
0	12	4	26.8	27.6	9		26.1	24.5	10		0.8*	4.2	0	5.5*	1.1	10	27.1	27.7		
1		2.2*	4.0	10		4.6*	8.1	8		20.2	20.7	0	4	6	64.8	64.6	11	8.0	8.1	
2		41.3	40.2	11		17.4	16.5	7		5.5	6.5	2	41.6	40.6	12	11	6	4.2*	8.7	
3		6.5*	8.6	12		0.9*	1.3	6		14.1	14.0	3	6.6*	1.6	11	5.5*	6.6			
4		26.1	25.2	13		6.5*	6.2	5		21.0	20.3	4	31.5	30.8	10	0.9*	1.9			
5		5.6*	5.1	14		2.5	2.5	4		11.7	10.0	5	6.7	6.8	9	0.9*	5.4			
6		2.7	20.1	15		0.9*	3.9	3		5.7	6.9	6	19.7	18.5	8	0.9*	5			
7		1.1*	1.0	16		8.5	8.3	2		6.0	6.7	7	4.9*	6.0	7	27.4	27.6			
8		24.9	23.5	11		1.8*	4.4	1		106.4	105.0	8	18.6	18.8	5	0.9*	2.5			
9		5.6*	6.6	10		15.4	15.5	0		0.5*	0.0	9	4.6*	3.5	5	16.5	18.1			
10		0.9*	4.4	9		20.7	20.5	0	1	5	0.4*	0.0	10	25.6	24.7	4	0.8*	3.8		
11		0.9*	0.8	8		15.1	14.5	1		23.0	22.4	11	0.8*	4.8	5	28.0	27.9			
10	13	4	1.9*	1.6	7		0.8*	2.2	2		104.7	105.1	12	8.7	9.6	2	0.8*	2.4		
9		25.7	24.6	6		21.5	21.6	3		8.8	8.8	13	0.9*	3.2	1	16.0	16.8			
8		0.9*	5.1	5		17.8	18.3	4		2.2*	2.5	14	3.0*	1.0	0	5.7*	3.5			
7		20.2	19.0	4		8.7	8.5	5		20.4	19.8	14	5	6	0.9*	4.0	12	6	0.9*	7.3
6		0.9*	2.4	3		5.5*	3.1	6		0.6*	1.5	13	22.9	23.2	2	4.4*	8.5			
5		2.5	21.5	21		0.7*	3.8	7		11.3	11.0	12	0.9*	1.9	2	31.7	31.4			
4		0.9*	1.5	1		10.2	11.4	8		15.1	14.8	11	32.8	31.2	3	7.7	7.7			
3		10.8	11.3	0		0.7*	0.0	9		20.1	19.8	10	0.8*	6.2	4	17.1	17.1			
2		0.9*	2.1	0	7	5	0.6*	0.0	10		19.9	19.6	9	22.4	21.1	5	0.9*	5.0		
1		29.8	28.9	2		29.4	28.4	11		10.0	11.5	8	4.4*	4.8	6	23.8	24.3			
0		2.8	2.4	2		4.9*	6.4	12		5.8*	6.4	7	19.2	19.2	2	3.9	2.6			
0	14	4	33.4	31.6	3		41.4	40.6	13		0.9*	6.4	6	7.2	7.5	8	22.6	22.2		
1		0.9*	4.0	4		36.1	35.3	14		11.4	12.4	5	4.2*	4.1	9	0.9*	4.1			
2		26.9	25.8	5		21.4	20.6	14	0	19.5	20.8	4	1.3*	4.4	10	14.5	15.4			
3		6.3*	2.2	6		14.8	13.8	13		5.3*	0.0	3	34.3	34.4	11	1.0*	2.8			
4		25.4	25.0	7		27.3	26.8	12		9.8	9.3	2	4.4*	4.7	9	13	6	3.2*	6.8	
5		0.9*	1.6	8		2.9*	5.8	11		0.8*	0.0	1	57.8	57.0	8	0.9*	2.1			
6		0.9*	8.0	9		4.4*	7.7	10		31.1	30.0	0	0.6*	0.9	7	20.0	19.4			
7		5.1*	8.7	10		11.0	11.4	9		0.7*	0.0	6	9.9	10.2	5	0.9*	1.3			
8		10.8	12.2	11		11.4	14.4	8		15.9	15.9	1	0.6*	2.3	5	20.2	20.1			
9	14	5	11.0	11.5	12		0.9*	2.0	7		1.4*	0.0	2	0.6*	2.2	4	5.4*	7.6		
7		0.9*	1.1	13		0.9*	2.2	6		47.1	45.1	3	0.6*	0.6	3	13.2	15.8			
6		14.7	14.2	14		0.9*	5.1	5		6.3*	0.0	4	37.3	37.4	2	0.9*	4.3			
5		3.8*	5.4	14		2.5*	4.3	4		21.6	19.9	5	0.7*	1.2	1	19.0	19.8			
4		14.2	12.1	13		0.9*	4.3	3		5.0*	0.0	6	26.2	26.7	0	11.1	11.4			
3		22.2	22.0	12		18.9	17.5	2		15.4	15.7	7	1.0*	5.7	0	14	6	23.9	23.9	
2		0.9*	4.6	11		0.8*	0.3	1		0.4*	0.0	8	12.7	12.8	1	0.9*	2.9			
1		0.9*	8.1	10		12.0	11.0	0		0.6*	0.0	9	10.5	5.2	2	17.8	17.9			
0	13	5	2.2*	0.0	9		22.4	22.9	0	0	68.6	70.7	10	26.8	26.5	3	0.9*	3.6		
1		0.9*	0.0	8		24.7	24.0	4		0.5*	0.4	11	0.8*	1.7	4	27.2	27.7			
2		9.1	12.9	2		13.6	14.4	2		102.1	102.6	12	19.1	19.1	5	0.9*	2.4			
3		6.5*	5.8	6		12.8	14.2	3		0.6*	0.0	13	0.9*	2.8	6	0.9*	4.4			
4		6.9*	8.5	5		33.1	32.8	4		84.1	84.9	14	12.6	12.3	7	0.9*	2.6			
5		0.9*	4.9	4		19.2	19.2	5		0.6*	0.0	14	7.6	5.5*	2.2	8	1.0*	8.0		
6		15.0	15.9	3		19.7	20.1	6		52.8	51.4	13	6.9*	7.3	7	3.1*	1.3			
7		0.9*	2.9	2		15.3	14.2	7		5.0*	0.0	12	0.9*	5.0	6	12.4	13.6			
8		0.9*	4.8	1		0.6*	2.7	8		14.8	15.8	11	8.8	7.4	5	4.8*	6.5			
9		0.9*	0.9	0		0.6*	0.0	9		0.7*	0.0	10	0.8*	3.6	4	9.3	8.8			
10		10.5	13.7	5	5	0.7*	0.0	10		27.5	27.3	9	37.8	36.9	3	8.2	9.5			
11	12	5	11.7	12.2	2		28.4	26.9	12		16.1	16.7	7	15.3	16.1	1	29.3	29.2		
10		7.7	7.5	4		19.9	19.9	17		0.9*	0.0	6	7.4	7.1	0	0.9*	0.0			
9		12.2	12.2	5		25.6	24.8	14		8.1	7.5	5	35.3	35.7	0	13	7	0.9*	0.0	
8		0.9*	0.9	6		32.6	32.7	16	1	4.3*	2.0	4	0.4*	5	1	4.4*	3.2			
7		6.3*	10.3	7		9.5	8.8	12		0.8*	1.2	2	33.3	33.3	2	10.3	10.5			
6		0.9*	4.5	8		17.0	17.3	11		14.3	14.2	1	6.1	6.9	4	0.9*	3.8			
5		16.6	16.5	9		16.3	17.2	10		4.4*	5.6	0	4.6*	3.3	5	18.7	19.9			
4		11.4	12.0	10		0.8*	2.8	9		0.7*	6.2	0	8	51.8	53.1	6	0.9*	1.0		
3		0.8*	2.6	11		6.5*	8.6	8		0.7*	2.7	1	5.2*	2.4	7	5.5*	4.5			
2		0.8*	1.7	12		0.8*	2.4	7		48.5	49.3	2	22.5	23.5	8	1.0*	1.3			
1		0.8*	0.0	13		7.6	8.3	6		0.6*	2.4	3	5.6	4.9	9	15.8	16.1			
0	11	5	0.8*	0.0	14		3.0*	7.1	5		47.5	44.8	4	13.6	12.7	10	12	7	1.0*	2.6
1		15.8	15.7	14	4	5	12.1	12.1	4		0.5*	0.8	5	0.7*	2.8	9	10.1	10.5		
2		21.6	21.2	12		2.9*	5.7	2		7.2	7.7	7	7.5	8.7	6	3.2*	4.7			
3		4.9	7.7	11		8.1	10.0	1		41.4	40.9	8	8.8	8.6	6	10.0	10.6			
4		13.8	15.2	10		30.6	29.3	0		16.5	16.5	9	0.8*	2.7	5	0.9*	0.8			
5		0.8*	0.5	9		5.4*	4.6	0	0	3.4*	0.5	9	19.3	18.4	4	0.9*	3.5			
6		16.3	12.6	0	3	5	1.1*	0.0	10		0.8*	1.0	8	0.8*	2.0	5	16.9	17.0		
7		21.2	20.0	8		0.7*	1.8	1		2.1*	3.3	11	0.9*	3.3	3	14.1	12.5			
8		7.5	8.0	7		29.3	28.5	2		78.9	79.8	12	26.1	24.5	2	7.5	6.1			
9		4.9*	3.0	6		38.2	38.9	3		4.2*	4.4	13	0.9*	2.4						

Table 3A. (Continued)

\bar{h}	\bar{k}	\bar{l}	F_{o}	F_{c}	\bar{h}	\bar{k}	\bar{l}	F_{o}	F_{c}	\bar{h}	\bar{k}	\bar{l}	F_{o}	F_{c}	\bar{h}	\bar{k}	\bar{l}	F_{o}	F_{c}
5	10	7	5.5*	8.2	7	3	7	37.0	36.6	12	3	8	4.3*	3.0	0	10	8	24.0	23.8
4			5.2*	5.3	8			15.5	15.7	11			9.1	8.5	1			7.0	7.2
3			5.3*	5.9	9			21.9	21.5	10			6.8	7.5	2			40.9	41.9
2			7.1	7.6	10			0.8*	5.2	9			22.1	21.1	3			10.1	10.6
1			27.7	27.0	11			29.7	29.5	8			0.7*	1.7	4			30.4	30.7
0			0.8*	0.0	12			0.9*	7.3	7			29.1	29.0	5			0.8*	3.0
9	9	7	0.7*	0.0	13			0.9*	14.6	6			4.2*	4.9	6			30.4	29.6
2			0.7*	0.3	14	2	7	6.2*	6.4	4			9.5	10.3	7			0.9*	4.7
3			11.9	11.6	15			11.9	15.0	3			5.4	6.3	8			18.4	18.5
4			27.2	26.9	12			34.2	34.6	2			6.7	6.2	10			20.7	20.6
5			40.2	40.1	11			35.4	34.5	1			23.9	23.3	11			0.9*	5.7
6			21.0	20.9	10			0.8*	2.8	0			12.2	11.9	12			8.5	11.1
7			13.6	14.1	9			0.7*	2.5	0	4	8	126.0	130.7	11	11	8	7.2*	5.6
8			7.3	8.8	8			33.3	33.8	1			4.7*	4.5	10			0.9*	3.9
9			29.8	29.4	7			9.0	10.2	2			40.4	39.5	9			2.0*	7.5
10			4.4*	7.1	6			8.8	9.6	3			0.6*	1.7	8			0.9*	2.8
11			20.6	21.5	5			1.5*	4.4	4			66.4	64.9	7			24.0	24.4
12			0.9*	3.1	4			33.5	33.6	5			0.9*	3.0	6			5.1*	5.4
13	8	7	15.6	16.8	3			42.9	41.3	6			20.7	21.8	5			12.2	11.4
2			5.0*	2.5	2			8.5	6.6	7			4.4*	3.8	8			3.5*	6.8
12			5.7*	5.0	5			47.0	44.3	9			4.2*	3.8	10			1.4*	9
11			0.9*	4.7	0			0.5*	0.0	9			8.3	9.2	2			0.8*	6.1
10			10.3	11.4	0	1	7	0.5*	0.0	10			22.1	22.5	1			14.4	14.4
9			4.0*	8.1	1			12.6	12.5	11			0.8*	2.5	0			0.9*	5.4
8			24.4	23.3	2			46.8	44.0	12			32.7	32.3	0	12	8	21.5	21.8
7			15.2	17.4	3			15.9	14.9	13			4.4*	5.6	1			0.9*	5.5
6			15.9	16.6	4			23.3	22.2	14			12.2	13.3	2			21.3	19.8
5			0.7*	4.5	5			27.9	27.1	14	5	8	3.9	2.5	3			0.9*	3.9
4			6.0	6.8	6			0.6*	3.9	13			21.9	23.0	4			30.0	29.4
3			19.0	18.1	7			27.1	27.5	12			0.9*	2.9	5			2.7*	0.0
2			15.5	16.3	8			0.7*	4.1	11			15.2	15.0	6			15.7	15.2
1			0.7*	2.9	9			36.0	34.1	10			4.6*	5.0	1			5.1*	4.9
0	7	7	0.7*	0.0	10			28.1	29.0	9			2.8*	4.4	8			0.9*	2.5
0	7	7	0.8*	0.0	11			20.9	21.0	8			2.3*	3.4	9			6.6*	6.0
1			31.2	31.4	12			9.1	10.5	7			2.7*	1.1	10			1.0*	8.4
2			13.9	15.1	13			14.7	15.6	6			10.4	10.4	9	13	8	11.7	12.0
4			11.7	11.4	14			21.1	22.1	5			25.7	25.7	8			1.0*	3.7
5			18.0	17.8	14	0	7	21.0	21.2	4			2.3*	2.3	7			12.8	15.0
6			22.3	22.2	13			0.9*	0.0	3			20.1	18.9	6			0.9*	1.8
7			31.8	32.1	12			7.3	8.2	2			5.7	5.9	5			24.4	24.2
8			25.5	24.5	11			0.8*	0.0	1			17.4	16.7	4			0.9*	1.4
9			8.9	7.8	10			39.4	39.9	9			4.6*	5.5	3			22.9	22.2
10			2.7*	5.2	9			0.7*	0.0	6	8		36.5	37.8	2			0.9*	2.4
11			18.7	19.3	8			15.0	16.6	1			4.4*	1.5	1			1.5	1.5
12			0.9*	2.0	7			0.7*	0.0	2			2.6*	2.9	0	14	8	10.3	11.6
13			19.9	19.6	6			51.5	50.0	3			20.6	18.9	6	12	9	18.5	19.6
14	6	7	1.0*	0.8	5			0.6*	0	4			18.9	19.4	1			4.7*	6.2
15			0.9*	0.8	3			0.6*	1.1	5			0.7*	3.1	2			13.9	15.4
16			9.5	8.7	2			28.1	27.3	7			0.7*	2.1	4			20.6	22.0
17			3.4*	4.7	1			0.5*	0.0	8			0.8*	2.6	5			0.9*	0.7
18			23.3	21.8	0			39.9	38.0	10			33.7	32.5	1			11.7	11.5
9			16.6	18.2	0	0	8	9.1	9.0	9			0.8*	2.8	2			1.0*	1.5
8			25.3	24.8	1			1.7*	0.0	12			27.5	27.6	6	14	9	5.1*	7.9
7			17.2	16.9	2			53.8	53.8	13			0.9*	1.1	5			0.9*	1.3
6			16.9	17.1	3			2.5*	0.0	14			9.5	10.6	4			0.9*	6.2
5			25.2	24.4	4			115.5	120.7	13	7	8	5.8*	2.3	3			5.4*	9.6
4			11.1	11.5	5			3.5*	1.1	12			0.9*	3.0	1			0.9*	5.1
3			31.0	31.1	6			2.8*	22.3	12			0.9*	3.5	2			12.2	12.9
2			9.2	9.9	7			0.7*	0.0	11			16.0	16.2	0			1.0*	0.0
1			0.6*	4.4	8			39.9	38.0	10			2.0*	3.8	8			8.3	8.1
0			0.6*	0.0	9			0.7*	0.0	9			33.7	32.5	1			3.2*	0.0
9	5	7	0.6*	0.0	10			21.4	21.7	8			0.8*	2.8	2			4.5*	1.5
1			32.2	31.9	11			0.8*	0.0	7			28.2	27.3	3			0.9*	5.9
2			6.1	5.2	12			11.3	10.1	6			9.5	9.5	4			5.7*	2.2
3			14.1	13.6	13			0.9*	0.0	5			14.4	15.4	5			9.7	10.2
4			29.7	30.1	14	1	8	11.0	14.6	4			4.0*	3.5	6			0.9*	6.1
5			50.7	51.1	14			7.0*	4.0	3			42.8	42.7	7			1.0*	3.9
6			26.0	26.1	15			13.3	13.6	2			0.8*	2.0	8			8.3	8.1
7			14.9	14.4	12			5.1*	1.6	12			10.6	10.9	12	9		2.0*	6.3
8			13.5	13.2	11			16.5	16.6	0			0.0*	1.1	8			1.6	1.7
9			33.4	32.8	10			2.5*	3.9	8	8		52.3	50.6	7			0.9*	4.3
10			7.3	9.0	9			6.8	8.2	1			0.7*	0.5	6			0.0*	3.5
11			17.4	17.5	8			1.7*	1.0	2			17.6	17.5	5			0.9*	2.0
12			0.9*	2.2	7			34.9	34.8	3			3.3*	6.7	4			11.5	12.1
13			23.0	23.1	6			0.6*	1.9	4			37.8	36.6	5			0.9*	3.9
14	4	7	7.2	6.7	5			26.9	25.9	5			4.4*	9.5	2			2.5*	6.2
15			0.9*	1.8	3			3.4	5.2	6			15.8	15.6	1			7.5	7.4
16			0.9*	4.4	2			24.4	24.7	7			2.4*	3.7	0			4.7*	0.0
17			0.8*	4.7	1			6.3	8.0	8			38.0	37.1	0	11	9	3.4*	0.0
18			27.5	27.0	7			1.7*	3.0	9			5.0*	1.4	10			12.8	12.6
19			26.8	26.															

Table 3A. (Continued)

h	k	l	F _o	F _c	h	k	l	F _o	F _c	h	k	l	F _o	F _c	h	k	l	F _o	F _c		
10	3	9	30.4	30.7	9	3	10	7.9	8.0	4	10	10	35.6	35.1	9	9	11	28.5	28.1		
11	-	-	10.7	8	5.3*	5.7	-	5	6.1*	8.8	10	-	-	14.9	15.4	2	2	11	31.1	30.9	
12	-	0.9*	1.2	7	10.3	19.5	-	6	27.0	26.9	11	-	-	0.9*	1.0	1	-	-	8.0	9.8	
13	-	0.9*	6.3	6	5.2*	2.6	-	7	0.9*	3.1	12	8	11	10.2	11.5	0	-	-	13.5	13.5	
14	-	14.9	15.8	5	24.5	24.0	-	8	24.6	24.5	11	-	-	11.9	11.5	0	1	11	7.5	0.0	
14	2	9	4.3*	5.8	4	5.4	7.0	9	0.9*	5.6	10	-	-	7.0*	11.6	1	-	-	25.7	25.5	
15	-	8.8	8.2	3	47.5	47.4	-	10	1.0*	7.3	9	-	-	14.1	14.8	2	-	-	20.6	19.8	
12	-	19.7	20.8	2	6.8	5.4	-	11	0.9*	5.2	8	-	-	3.5*	6.5	3	-	-	13.5	13.5	
11	-	0.8*	4.8	1	0.6*	2.4	-	10	11	10	5.9*	4.4	7	4.1*	6.9	4	-	-	35.1	34.4	
10	-	10.2	10.3	0	1.6*	1.3	-	9	-	-	6.7*	6.7	6	9.7	9.6	5	-	-	18.7	19.5	
9	-	30.6	29.3	0	4	10	95.3	95.8	8	1.6*	3.2	5	-	-	10.8	17.1	7	-	-	19.8	19.4
8	-	36.5	35.2	1	6.3	5.7	-	7	16.0	20.0	4	-	-	10.8	17.1	8	-	-	20.6	20.3	
7	-	4.3*	6.6	2	46.0	46.0	6	-	0.9*	3.5	5	1.1*	2.8	14	-	-	1.8*	4.1	-		
6	-	13.2	13.1	3	5.0*	4.5	5	13.3	14.3	2	-	-	0.8*	2.3	9	-	-	20.6	20.6		
5	-	31.9	32.2	4	47.7	45.8	4	1.5*	5.1	1	-	-	28.9	27.5	10	-	-	0.8*	2.5		
4	-	35.6	35.5	5	1.8*	2.7	3	23.7	23.1	0	-	-	0.8*	0.0	11	-	-	20.8	20.9		
3	-	17.2	16.8	6	12.1	11.2	2	-	0.9*	2.5	0	7	11	3.3*	0.0	12	-	-	5.4*	2.2	
2	-	4.1*	5.0	7	4.1*	7.3	1	11.4	12.8	1	-	-	18.0	17.5	15	-	-	17.3	18.5		
1	-	43.3	42.5	8	11.0	9.5	0	-	0.8*	1.7	2	-	-	24.5	22.8	14	-	-	1.8*	4.1	
0	-	0.6*	0.0	9	6.6	6.3	0	12	10	24.9	22.8	5	-	-	27.3	28.2	14	0	11	9.2	12.6
0	1	9	0.6*	0.0	10	17.7	17.5	1	-	0.9*	3.4	4	-	-	0.8*	4.3	15	-	-	0.9*	0.0
1	-	16.0	15.4	11	4.9*	5.7	2	40.3	40.6	5	-	-	8.3	7.0	12	-	-	6.4*	9.2		
2	-	39.9	39.4	12	22.1	22.7	3	-	2.1*	5.8	6	2.4*	4.1	11	-	-	0.9*	0.0	-		
3	-	6.8	6.3	13	1.7*	3.5	4	19.2	19.1	7	-	-	32.0	31.5	10	-	-	23.5	24.1		
2	-	21.5	16.0	14	18.5	19.8	5	-	7.3	7.6	8	1.2*	8.1	9	-	-	7.8*	0.0	-		
5	-	16.4	15.3	14	5	10	0.9*	2.9	6	16.3	17.0	9	-	-	15.2	16.9	8	-	-	7.4*	8.1
6	-	11.2	11.5	13	0.9*	3.3	3	4.8*	8.7	10	-	-	9.1	9.4	7	-	-	7.7*	0.0		
7	-	1.8*	4.9	12	0.9*	2.8	8	10.3	11.8	11	-	-	14.3	13.5	6	-	-	31.0	31.1		
8	-	0.7*	2.5	11	12.7	13.2	9	0.9*	3.0	12	-	-	0.9*	3.7	5	-	-	0.7*	0.0		
9	-	7.8	10.2	10	4.5*	7.8	8	15	10	5.7*	2.3	15	1.0*	6.0	4	-	-	6.2	7.7		
10	-	0.8*	3.1	9	30.2	29.9	7	-	11.0	10.9	13	6	11	0.9*	6.4	3	-	-	3.2*	0.0	
11	-	7.3	8.0	8	0.8*	3.5	6	-	0.9*	6.3	12	-	-	13.3	14.2	2	-	-	4.9*	6.2	
12	-	0.9*	3.5	7	5.5*	5.7	5	-	20.8	22.1	11	-	-	18.5	18.1	1	-	-	3.2*	0.0	
13	-	0.9*	4.5	6	0.7*	2.7	4	-	3.0*	3.5	10	-	-	7.4	9.2	0	-	-	0.8*	0.0	
14	-	10.4	12.2	5	49.4	49.1	1	-	29.7	29.8	9	-	-	7.8	10.6	0	0	12	106.0	108.2	
14	0	9	17.0	19.6	4	7.3	7.4	2	-	14.1	14.2	1	-	-	17.7	17.2	1	-	-	0.6*	0.0
13	-	0.9*	0.0	3	17.0	15.4	1	-	8.0	11.9	7	-	-	5.0*	6.2	2	-	-	50.0	49.1	
12	-	7.1	8.9	2	6.4	5.0	-	-	6.0*	9.3	6	-	-	2.5*	4.9	5	-	-	7.7*	0.0	
11	-	0.8*	0.0	1	42.7	43.3	0	14	27.6	27.6	5	-	-	0.8*	2.3	4	-	-	6.1	5.7	
10	-	25.1	23.4	0	13.1	12.3	1	-	14.1	12.6	0	5	11	20.2	19.7	5	-	-	3.4*	0.0	
9	-	0.8*	0.0	6	10	20.9	22.0	2	-	15.8	16.1	3	-	-	22.1	20.9	6	-	-	0.8*	3.7
8	-	22.4	22.7	1	0.7*	0.6	3	-	0.9*	5.7	2	-	-	0.7*	0.6	7	-	-	0.8*	0.0	
7	-	0.7*	0.0	2	32.5	31.0	4	-	19.0	17.9	1	-	-	16.3	15.8	8	-	-	41.2	40.1	
6	-	35.5	36.0	3	0.7*	4.1	5	-	1.0*	5.2	0	-	-	0.7*	0.0	9	-	-	0.8*	0.0	
5	-	3.2*	0.0	4	36.6	36.1	6	-	13.1	12.6	0	5	11	22.0	19.7	5	-	-	11.1	14.2	
4	-	14.4	14.8	5	4.1*	3.4	5	-	14.2	14.0	1	-	-	35.8	36.5	11	-	-	51.8	55.4	
3	-	0.7*	0.0	6	22.7	22.8	4	-	3.2*	2.7	2	-	-	11.2	11.5	12	-	-	22.6	22.5	
2	-	17.6	16.6	3	0.8*	3.9	7	-	1.0*	5.0	5	-	-	8.5	6.8	8	-	-	0.9*	0.0	
1	-	1.6*	0.8	8	15.7	15.0	9	-	6.0*	7.4	4	-	-	16.5	17.2	14	-	-	6.2	6.0	
0	-	0.7*	0.0	9	2.2*	3.2	1	-	1.0*	5.6	5	-	-	30.2	30.0	10	1	12	0.9*	2.6	
0	0	10	49.8	48.9	10	11.2	12.6	0	-	0.9*	0.0	6	-	-	0.8*	1.5	13	-	-	5.4*	9.2
1	-	0.6*	0.0	11	0.9*	3.2	0	13	11	0.9*	0.0	7	-	-	15.6	15.3	12	-	-	0.9*	1.7
2	-	44.6	44.9	12	10.2	9.7	1	-	19.6	21.7	8	-	-	7.7	9.0	11	-	-	13.8	14.9	
3	-	1.2*	0.0	13	1.0*	4.1	2	-	6.5*	1.9	9	-	-	32.4	32.2	10	-	-	0.8*	2.8	
4	-	46.0	44.2	14	4.4*	7.6	3	-	10.2	8.2	10	-	-	9.5	10.2	9	-	-	16.3	16.1	
5	-	5.1*	0.0	13	5.4*	4.9	3	-	10.4	11.4	11	-	-	8.5	6.8	8	-	-	3.1*	5.3	
6	-	19.4	18.9	12	0.9*	2.1	5	-	7.4*	10.6	12	-	-	7.4	6.5	7	-	-	14.3	15.4	
7	-	0.7*	0.0	11	12.6	7	-	-	9.2	9.2	14	-	-	9.5	10.8	6	-	-	4.1*	3.3	
8	-	38.0	36.9	10	0.9*	3.1	1	-	11.1	11.6	4	-	-	5.6*	9.0	5	-	-	7.2	7.5	
9	-	0.8*	0.0	9	30.1	29.6	8	12	11	11.6	11	-	-	-	10.8	12.8	4	-	-	8.0	7.5
10	-	7.4	8.5	8	2.7*	4.0	7	-	4.5*	4.7	15	-	-	12.4	14	5	-	-	8.8	9.2	
11	-	2.4*	0.0	7	17.1	16.8	2	-	6.0*	1.9	12	-	-	8.0	11.1	2	-	-	6.2	5.9	
12	-	9.0	7.8	6	6.7	4.3	5	-	6.7*	7.1	11	-	-	13.1	14.5	1	-	-	21.0	20.8	
13	-	0.9*	0.0	5	30.1	29.9	4	-	14.1	14.4	1	-	-	25.2	25.1	0	-	-	5.6	5.7	
14	-	16.9	20.1	4	2.0*	5.7	10	11.0	11	5.5*	7.0	5	-	-	7.6*	8.7	1	-	-	35.1	34.7
15	-	1.4*	0.0	8	34.4	34.1	2	-	10.5	11.2	6	-	-	17.8	18.3	4	-	-	7.1	8.1	
16	-	0.8*	0.0	10	26.7	26.5	1	-	1.1*	6.6	4	-	-	10.5	10.2	5	-	-	37.8	36.9	
17	-	0.8*	5.1	1	4.8*	1.8	2	-	6.4*	7.6	5	-	-	27.6	27.6	6	-	-	37.8	36.9	
18	-	0.7*	1.1	2	15.0	15.9	3	-	20.2	20.3	2	-	-	5.4*	6.8	7	-	-	7.8	7.5	
19	-	14.5	13.9	3	0.5	6.4	4	-	14.0	13.4	1	-	-	31.6	30.9	8	-	-	14.0	14.0	
20	-	3.8*	7.9	4	28.7	28.4	5	-													

Table 3A. (Continued)

h	k	l	F_o	F_c	h	k	l	F_o	F_c	h	k	l	F_o	F_c	h	k	l	F_o	F_c
6	4	12	19.5	19.2	1	6	12	1.9*	4.1	2	7	12	0.8*	2.7	4	9	12	0.8*	4.8
7			0.8*	5.2	2			40.2	38.9	1			20.3	19.2	3			0.9*	4.8
8			23.9	23.2	3			0.8*	5.4	0			6.3	5.9	2			0.9*	2.0
9			5.0*	5.6	4			10.1	10.1	0	8	12	37.3	36.8	1			14.1	15.1
10			24.0	23.3	5			2.9*	3.2	1			2.7*	2.9	0			8.0	8.6
11			0.9*	7.3	6			48.5	46.3	2			9.1	10.4	0	10	12	15.9	16.0
12			8.8	10.6	7			0.8*	2.9	3			5.0*	3.5	1			0.8*	3.3
13			6.2*	7.4	8			22.1	22.1	4			29.8	29.3	2			11.8	10.9
15	5	12	9.4	8.9	9			0.9*	2.6	5			1.6*	3.4	3			0.9*	4.5
12			8.3	7.9	10			20.7	20.2	6			8.9	11.0	4			4.9*	5.8
11			19.5	21.2	11			0.9*	3.4	7			0.9*	4.3	5			0.9*	6.4
10			4.9*	5.6	12			0.8*	2.0	8			11.8	12.7	6			18.9	18.2
9			21.3	20.9	13			0.9*	3.7	9			9.5	9.8	7			8.8	9.7
8			0.8*	2.9	12	7	12	2.5*	5.2	10			9.9	12.5	8			0.9*	4.0
7			48.4	47.6	11			0.9*	3.9	11			7.8	10.5	9			5.1*	8.2
6			4.7*	5.1	10			0.9*	4.2	12			7.3*	11.1	10			1.0*	2.1
5			0.8*	2.8	9			19.2	19.9	11	9	12	12.8	13.7	9	11	12	7.6	8.6
4			0.7*	4.5	8			0.9*	3.5	10			0.9*	4.9	8			1.0*	4.1
3			0.7*	3.1	7			10.4	7.5	9			13.3	13.8	7			2.7*	7.3
2			0.7*	4.2	6			0.8*	1.6	8			0.9*	2.7	6			7.8	7.8
1			1.8*	2.4	5			45.7	45.8	7			8.9	9.1	5			8.2	7.7
0			8.1	7.2	4			0.8*	3.1	6			4.7*	6.8	4			0.9*	2.1
0	6	12	11.9	12.9	3			18.6	19.0	5			15.2	16.5	3			10.4	11.7

Description of the structure

The structure was described by ITO *et al.* (1951) as being a "three-dimensional unbroken boron-oxygen network with magnesium and chlorine atoms filling the interstices". This description is correct, and we are merely revising its details, which are, however, important in respect to both crystal-chemical and physical properties.

The boron-oxygen network

This network actually has three normal tetrahedra linked at a common oxygen atom. Three more tetrahedra share corners to form three six-membered boroxol rings. The ring system is linked to other equivalents by further corner-sharing, involving oxygen atoms of symmetry-related tetrahedra and of a single boron-oxygen triangle. The asymmetric unit of the orthorhombic structure (which also appears in the trigonal structure) is illustrated schematically in Fig. 1 and as it appears in the orthorhombic structure in Fig. 2. One triangular boron atom, B(3), is 2.30 Å distant from the oxygen atom O(1) that is linked to three tetrahedral boron atoms of the B(2) group, and these four boron atoms correspond to the four boron atoms of the "BO₃O pyramids" originally described in the cubic structure (ITO *et al.*, 1951). The refinement of the lower-symmetry structures, however, shows that in these two structures the distances and angles are normal for tetrahedra and triangle (Tables 5 and 6)². The 2.30 Å approach, which reaches 2.42 Å in the iron-rich analogue, is much too long to be considered a

² Distances and angles are given for boracite only, except in Tables 9 and 10, as the values for the borate framework of the iron-rich analogue agree within the limits of error with the average values for boracite.

Table 3. Comparison of observed and calculated structure factors.
B. Iron-rich analogue of boracite. * indicates "less-than" reflections

h	k	l	F_o	F_c	h	k	l	F_o	F_c	h	k	l	F_o	F_c	h	k	l	F_o	F_c			
3	0	0	210.4	207.6	14	1	1	4.8*	12.1	1	1	3	2.0*	4.7	7	2	5	3.5*	7.7			
6			241.0	231.4	13	0	1	4.6*	0.0	4	2.6*	12.1	4	29.0	28.5	12	2	7	23.6*	24.6		
9			82.2	82.7	10			5.9*	0.0	7	3.4*	27.9	1	14.7*	22.3	9			4.0*	2.8		
12			54.2	49.9	7			5.1*	0.0	10	35.9	31.4	3	1.5	2.4*	13.0	6		5.4*	12.7		
15			48.6	46.9	4			2.4*	0.0	13	4.8*	11.5	6	5.1*	8.6	3			2.7*	16.2		
13	1	0	47.7	54.9	1			1.6*	0.0	15	0	5	4.4*	0.0	9	32.3	33.4	2	1	7	182.3	169.3
10			58.0	60.3	2	0	2	180.3	168.4	12	4.4*	0.0	12	4.5*	4.5	5			4.5*	4.6		
7			6.2	7.8	5			205.6	201.1	9	5.0*	0.0	15	4.8*	17.9	8			3.6*	8.8		
4			117.7	110.0	8			63.1	57.2	6	5.0*	0.0	14	0	5	4.8*	0.0	11			4.3*	11.5
1			62.8	55.0	11			84.9	82.3	3	5.8*	0.0	11	4.5*	0.0	14			5.0*	11.1		
2	2	0	278.7	318.8	14			40.2	33.4	1	0	4	116.6	111.2	8	14.5*	0.0	13	0	7	4.6*	0.0
5			109.0	120.2	15	1	2	4.9*	13.6	4	37.5	34.6	5	14.2*	0.0	10			6.1*	0.0		
8			64.2	67.0	12			37.3	23.9	7	136.6	130.0	2	2.1*	0.0	7			5.4*	0.0		
11			60.2	65.7	9			49.6	54.4	10	84.7	77.0	0	0	6	332.3	338.5	4			2.6*	0.0
14			42.6	48.0	6			56.5	45.0	13	92.9	82.7	6	121.3	121.6	1			6.4*	0.0		
12	3	0	47.7	13.4	3			67.9	63.0	14	1	4	4.8*	19.8	9	125.0	118.5	2	0	8	336.1	331.3
9			67.9	70.8	0			63.5	68.5	11	38.6	44.1	12	91.5	84.5	5			222.4	221.0		
6			80.2	80.7	1	2	2	194.1	206.6	8	61.6	53.6	15	36.0	34.8	8			107.2	102.5		
3			27.7	23.4	4			90.2	96.7	5	54.6*	55.4	1	1	6	35.1	28.5	11			48.1	49.4
0			184.2	215.2	7			150.1	168.4	2	58.1	21.6	10	67.6	59.3	14			25.1*	25.6		
1	4	0	109.9	119.9	10			4.9*	13.4	0	2	420.3	436.1	7	108.1	102.2	12	1	8	17.4	0.0	
4			142.9	157.1	13			15.9*	23.8	4	170.0	171.3	4	165.0	155.3	9			34.4	34.6		
7			88.3	95.5	11	3	2	16.1*	38.1	6	145.6	145.1	1	177.7	165.9	6			88.4	80.9		
10			48.5	50.8	8			45.7	54.9	9	101.0	93.0	2	2	268.0	223.1	3			37.7	23.9	
15			4.9*	19.9	5			39.3	47.2	12	28.8*	32.0	5	125.6	129.8	0			55.3	55.4		
11	5	0	54.5	58.4	2			191.1	210.6	13	3	4	54.9	45.1	8	3.8*	26.5	1	2	8	116.5	117.0
8			16.8*	16.4	0	4	2	207.1	227.3	10	21.5*	13.0	11	54.7	65.2	4			262.3	254.2		
5			90.9	96.5	3			96.4	107.3	7	76.9	75.7	14	47.7	45.3	7			148.1	142.4		
2			121.0	130.0	6			3.6*	24.4	4	115.4	121.3	12	3	6	4.8*	16.5	10			28.0	32.8
0	6	0	216.0	250.4	9			66.4	70.2	4	46.9	48.5	9	21.5*	45.3	15			4.9*	26.1		
3			83.5	79.6	12			8.1*	36.3	2	4	204.1	218.9	6	89.2	78.9	11	3	8	33.4	39.8	
6			77.6	60.3	10	5	2	4.7*	25.5	5	102.9	101.1	3	70.4	71.4	8			4.8*	40.6		
9			22.2*	35.5	7			88.0	90.0	8	26.2*	41.8	6	198.9	205.5	5			62.0	67.3		
10	7	0	4.9*	15.3	4			152.4	182.9	11	4.5*	38.7	1	4	6	126.9	150.0	2			139.8	131.6
2			119.1	112.1	1			67.1	70.2	12	5	4	4.8*	10.8	4	64.3	70.2	0	4	8	220.0	223.8
4			93.7	101.1	2	6	2	55.1	54.9	9	64.3	65.1	7	46.0	50.4	3			45.8	79.4		
1			67.0	76.0	5			69.5	71.0	6	56.1	50.5	10	41.7	47.4	6			70.1	67.3		
2	8	0	65.1	62.2	8			4.4*	18.8	3	95.2	102.1	13	4.4*	15.2	9			92.0	87.8		
5			33.5	33.0	11			36.7	36.0	0	175.5	190.7	11	5	6	63.0	56.3	12			25.4*	26.7
8			4.8*	1.4	9	7	2	12.8*	36.0	1	6	124.2	133.3	8	66.6	70.8	10	5	8	4.8*	6.9	
9	9	0	71.5	55.2	6			61.9	65.3	4	66.1	66.5	5	10.5*	53.3	7			85.1	84.7		
6			4.7*	30.4	3			16.8*	23.2	7	68.3	75.9	2	171.0	183.3	4			84.1	76.3		
3			78.3	76.4	0			140.5	138.6	10	4.7*	11.2	0	6	6	72.5	78.6	1			90.9	94.9
0			84.5	90.3	1	8	2	58.1	36.1	4	5.7	11.2	5	63.5	67.6	2	6	8	126.4	134.7		
1	10	0	69.7	59.9	4			54.2	52.2	5	5.4*	18.7	6	4.7*	26.5	8			77.1	75.7		
4			50.2	52.2	7			7.1	15.9*	3	119.3	129.0	9	4.7*	19.2	11			4.5*	19.9		
7			4.8*	15.3	10			10.3*	23.7	0	8	4	105.3	109.9	10	6	4.9*	26.5	8			
5	11	0	61.7	54.5	8	9	2	4.9*	25.0	3	56.7	54.4	7	62.8	65.8	9	7	8	68.1	62.6		
2			74.0	69.6	5			65.5	65.5	6	4.5*	14.0	4	112.5	113.3	6			58.2	66.3		
0	12	0	22.6*	41.9	2			96.0	101.0	9	5.0*	24.2	1	5.4*	5.0	5			36.1	42.2		
3			4.7*	13.4	0	10	2	32.0	26.7	7	9	4	74.0	70.9	2	8	6	171.0	155.0			
4	13	0	4.8*	22.8	3			35.4	31.7	4	4.4*	24.1	5	31.1	28.3	1	8	8	67.2	64.6		
1			57.4	54.9	6			33.0	38.8	1	76.3	80.4	8	4.8*	19.6	4			69.1	61.6		
2	14	0	45.4	42.2	4	11	2	59.1	53.4	2	10	60.1	57.9	6	62.3	59.8	7			19.2*	34.0	
0	15	0	50.2	47.2	1			4.5*	19.0	5	4.7*	15.5	3	57.5	63.7	8	9	8	4.0*	19.8		
1	15	1	4.8*	4.1	4	2	12	45.7	46.5	8	4.8*	9.3	0	112.9	111.0	5			63.5	57.5		
5	14	1	9.3*	16.1	1			5.9*	15.8	6	11.1	4	24.1*	26.6	1	10	6	4.4*	35.2	20.4		
2	15	1	6.6*	16.1	5	13	2	32.0	45.2	7	50.4	60.0	4	32.5	38.4	0	10	8	70.4	78.0		
1			8.5*	6.7	1	14	2	4.8*	17.4	1	12	32.2	31.9	5	11.6	6.2	2	27.7*	63.8	6		
3	11	1	30.2	33.6	2	13	2	20.1*	2.9	4	50.2	43.6	6	96.5	90.0	4	11	8	15.6*	22.5		
6			10.0*	11.9	13	3	4.7*	11.0	2	13	35.9	43.3	3	12	41.6	49.3	1			44.4	46.1	
8	10	1	4.8*	5.7	4			6.9*	9.7	0	14.4	19.4	3	4.7*	12.9	2	12	8	38.4	31.8		
5			4.6*	9.2	3	12	3	4.7*	5.0	1	15.1*	29.5*	2	4.7*	28.5	5			4.8*	14.5		
2			11.4*	16.1	2	11	3	4.5*	2.7	1	11.4*	5.0*	1	17.4*	22.4	3	15	8	47.8	41.7		
1	9	1	37.2	39.9	5			4.7*	4.4	3	13.3	5.4*	2	14	6.2	4.0*	6	35.8	39.5			
4			6.5*	7.8	7	10	3	4.9*	8.2	5	12.7*	5.1	1	35.8*	57.9	0			4.8*	13.0		
9	8	1	12.7*	8.1	1			4.1*	9.8	1	11.1	5	4.7*	21.5								

Table 3B. (Continued)

\mathbf{k}	\mathbf{k}	\mathbf{l}	F_o	F_c	\mathbf{h}	\mathbf{k}	\mathbf{l}	F_o	F_c	\mathbf{h}	\mathbf{k}	\mathbf{l}	F_o	F_c	\mathbf{h}	\mathbf{k}	\mathbf{l}	F_o	F_c
6	0	36	49.4	48.5	0	9	36	30.6*	37.0	6	1	38	4.8*	9.6	1	1	39	4.8*	11.5
9		47.2	42.5		2	7	37	4.8*	9.9	3			4.7*	14.3	4			4.9*	6.0
7	1	36	41.2	42.5	1	6	37	4.8*	4.7	0			4.6*	4.7	6	0	39	4.9*	0.0
4		44.3	43.4		3	5	37	4.7*	14.9	1	2	38	14.1*	35.4	3			4.8*	0.0
1		23.0*	36.2		5	4	37	4.8*	4.9	4			22.1*	34.5	1	0	40	4.8*	16.5
2	2	36	55.5	52.1	2			4.7*	10.7	5	3	38	4.8*	11.1	4			54.0	54.1
5		27.8*	22.9		1	3	37	23.2*	28.9	2			4.8*	36.0	5	1	40	4.8*	26.1
8		6.8*	5.1		4			4.8*	2.4	6	4	38	71.4	69.1	2			4.8*	23.8
6	3	36	41.5	50.9	6	2	37	4.8*	20.4	3			4.8*	4.5	0	2	40	50.8	27.2
3		4.7*	20.6		3			4.8*	4.5	4	5	38	20.8*	52.5	3			56.4	64.5
0		77.8	77.2		2	1	37	4.7*	14.9	1			4.8*	24.9	4	3	40	27.5*	12.2
1	4	36	19.5*	31.2	5			4.7*	11.5	2	6	38	4.9*	26.2	1			15.4	31.3
4		55.2	59.8		8			4.9*	12.4	0	7	38	50.4	56.0	2	4	40	45.3	66.8
5	5	36	31.9	32.4	7	0	37	4.7*	0.0	0	2	39	4.7*	10.2	0	5	40	67.1	70.0
2		17.6*	22.3		4			4.7*	0.0	4	4	39	4.7*	10.5	1	6	40	4.9*	26.2
0	6	36	37.4	46.7	1			4.6*	0.0	1			4.8*	20.1	1	5	41	4.8*	16.3
3		17.6*	22.3		2	0	38	35.2	35.3	3	3	39	4.7*	33.4	2	3	41	4.7*	9.4
1	7	36	0.6*	15.1	5			45.6	52.8	5	2	39	4.7*	0.6	4	2	41	4.7*	15.0
2	8	36	4.8*	11.1	8			26.2*	21.5	2			2.3*	29.2	1			4.8*	5.3

normal B—O bond. Undoubtedly this close approach does mean that small atomic shifts can cause a triangle to become a tetrahedron, while simultaneously, one of three tetrahedra becomes a triangle, thus contributing to the observed ferroelectricity and ferroelasticity (DOWTY and CLARK, 1972b). No major change in the remainder of the frame-work occurs during such "ferro" transitions, and afterwards the structure is exactly the same, only it has a different orientation.

The occurrence of three borate tetrahedra linked at corners by a common oxygen atom was first discovered in the structure of the mineral tunellite, $\text{SrB}_6\text{O}_9(\text{OH})_2 \cdot 3\text{H}_2\text{O}$ (CLARK, 1964). Since then, this feature has been found in the structures of three other hydrated borates: macallisterite, $\text{Mg}_2[\text{B}_6\text{O}_7(\text{OH})_6]_2 \cdot 9\text{H}_2\text{O}$ (DAL NEGRO *et al.*, 1969); strontioginorite, $\text{SrCaB}_{14}\text{O}_{20}(\text{OH})_6 \cdot 5\text{H}_2\text{O}$ (KONNERT *et al.*, 1970); and aksaite, $\text{MgB}_6\text{O}_7(\text{OH})_6 \cdot 2\text{H}_2\text{O}$ (DAL NEGRO *et al.*, 1971). In all of these structures, each of the three corner-linked tetrahedra participate in a ring system formed by further corner-sharing, each ring being composed of two tetrahedra and a triangle. The three-ring polyanion $[\text{B}_6\text{O}_7(\text{OH})_6]^{2-}$ occurs isolated in the structures of macallisterite and aksaite, whereas in tunellite and strontioginorite, the polyanions link to form infinite sheets. The structures of strontium and lead tetraborates (PERLOFF and BLOCK, 1966) and of B_2O_3 II (the high-pressure form, PREWITT and SHANNON, 1968) also have the feature of three tetrahedra linked at a common oxygen atom, but the ring unit does not occur in these structures. However, in all cases the B—O distances for the triply coordinated oxygen atom are the longest B—O bonds observed, in accordance with the discussion by ZACHARIASEN (1963). This rule is followed also for boracite and its iron-rich analogue. However, the average distance for the triply coordinated oxygen atom to its associated boron atoms is substantially longer in boracite and the

Table 4. *Magnitudes and orientations*

Ellipsoid axis, r_i	Cl	Mg(1)	Mg(2)	Mg(3)
Amplitude				
$i = 1$	0.10 Å	0.07 Å	0.07 Å	0.07 Å
2	0.11	0.07	0.09	0.07
3	0.11	0.11	0.11	0.11
Angle of r_i with				
a $i = 1$	97.5°	80.8°	129.2°	131.2°
2	75.8	170.4	104.5	95.3
3	16.1	87.2	137.2	41.7
b $i = 1$	19.0	12.4	43.1	131.0
2	71.2	81.4	82.9	114.5
3	156.2	98.8	132.2	129.1
c $i = 1$	16.1	81.8	75.0	68.4
2	87.3	85.8	163.7	154.8
3	74.1	9.2	84.0	77.7
Ellipsoid axis, r_i	O(2)-2	O(2)-3	O(2)-4	O(2)-5
Amplitude				
$i = 1$	0.04 Å	0.06 Å	0.06 Å	0.05 Å
2	0.08	0.07	0.07	0.07
3	0.08	0.08	0.09	0.10
Angle of r_i with				
a $i = 1$	114.8°	52.9°	74.6°	32.3°
2	141.1	40.4	162.9	122.3
3	62.1	76.1	97.2	89.3
b $i = 1$	104.9	133.9	29.0	57.8
2	113.1	69.5	72.9	32.4
3	152.1	51.0	112.8	86.4
c $i = 1$	29.5	66.7	66.0	92.5
2	119.4	123.1	90.4	92.7
3	92.0	42.3	24.0	3.7

anhydrous $\text{SrO} \cdot 2\text{B}_2\text{O}_3$ than in the other compounds where this coordination occurs, as shown by the average values compared in Table 7.

*of thermal ellipsoids in boracite**

B(1)-1	B(1)-2	B(1)-3	B(2)-1	B(3)	O(1)	O(2)-1
0.03 Å	0.06 Å	0.07 Å	0.03 Å	0.06 Å	0.05 Å	0.04 Å
0.04	0.06	0.08	0.06	0.07	0.07	0.07
0.08	0.10	0.09	0.11	0.10	0.09	0.08
78.5°	31.8°	90.8°	79.6°	67.2°	112.0°	31.2°
132.8	106.0	21.2	11.8	122.1	135.4	61.3
134.9	116.7	68.9	84.6	138.9	126.4	101.4
51.7	62.3	166.3	156.8	143.0	22.8	70.9
49.8	37.5	95.6	82.3	127.0	102.6	142.6
116.5	66.8	77.5	68.3	89.2	108.7	120.8
40.6	75.6	76.3	69.5	62.5	84.3	66.3
110.4	122.9	110.3	98.9	126.6	131.9	111.9
56.7	36.7	24.9	22.5	48.9	42.4	33.3
O(2)-6	O(2)-7	O(2)-8	O(2)-9	O(2)-10	O(2)-11	O(2)-12
0.06 Å	0.04 Å	0.04 Å	0.02 Å	0.05 Å	0.06 Å	0.06 Å
0.08	0.06	0.09	0.06	0.06	0.06	0.07
0.09	0.09	0.10	0.08	0.08	0.08	0.09
55.7°	99.3°	79.2°	91.2°	74.6°	80.8°	84.4°
125.6	51.4	169.2	78.4	68.3	98.8	138.3
125.9	40.1	90.8	11.7	27.1	12.8	131.2
145.0	71.2	167.3	54.1	124.8	76.6	12.4
107.4	40.0	100.8	37.3	133.1	162.7	78.5
119.3	123.8	83.5	98.7	63.0	100.8	94.7
96.3	21.2	83.5	36.0	39.1	16.3	78.9
139.1	99.0	89.5	124.8	129.0	75.2	129.4
49.8	71.0	6.5	82.2	88.3	96.8	41.6

* Non-positive definite for B(2)-2,3.

In boracite, due to the corner-linking of three tetrahedra to form a six-membered boroxol ring, the ring is substantially more distorted than for those compounds in which it is formed from linkages of two

Table 3B. (Continued)

h	k	l	F_o	F_c	h	k	l	F_o	F_c	h	k	l	F_o	F_c	h	k	l	F_o	F_c			
12	3	9	4.9*	2.0	11	3	11	4.8*	23.2	12	2	13	4.8*	8.9	4	1	15	29.0	32.0			
14	2	9	4.8*	5.0	13	2	11	4.9*	7.7	9	4.5*	16.3	50.0	39.0	6	14.5	137.0	40.8	38.6			
11	1	2	14.2	14.1	10	4.5*	4.9	6	24.4	28.2	10	4.4*	13.7	9	74.6	26.8						
8			36.5	35.0	7	14.8*	7.4	3	29.6	37.8	13	4.9*	7.2	12	73.1	62.5						
5			7.2*	18.5	4	14.1*	24.4	2	1	13	69.6	57.6	12	0	15	4.7*	0.0	13	1	18	39.6	45.2
2			66.7	67.3	5	1	73.5	73.8	5	44.9	44.7	9	4.1*	0.0	10	45.3	39.5					
1	1	9	160.7	153.3	3	1	11	59.6	61.3	8	23.0*	36.3	3	0	18	40.8	38.6					
4			50.9	48.3	6	21.7	11.1	11	4.5*	6.0	3	3.0*	0.0	4	95.4	86.3						
7			4.5*	11.1	11	4.0*	13.7	14	4.9*	3.2	1	0	16	152.0	135.5	1	2	2	18	67.4	58.5	
10			4.2*	6.5	9	4.7*	15.1	13	0	13	4.9*	0.0	4	137.0	132.0	2	2	18	163.5	168.8		
13			4.8*	18.6	14	0	11	4.8*	0.0	10	4.4*	0.0	7	33.2	1	129.1	5	81.2	79.2			
15	0	9	4.9*	0.0	11	4.8*	0.0	7	3.5*	0.0	10	4.4*	19.5	8	61.4	59.7						
12			2.9*	0.0	8	3.7*	0.0	4	3.0*	0.0	13	4.5*	4.9	11	3.5*	26.0						
9			5.1*	0.0	5	3.1*	0.0	1	10.6*	0.0	14	1	16	4.9*	7.9	12	3	18	4.9*	13.4		
6			5.2*	0.0	2	12.4*	0.0	2	0	14	231.6	230.7	11	35.1	43.8	9	60.4	62.6				
3			2.5*	0.0	0	0	12	305.6	296.3	5	65.8	67.7	8	48.7	37.3	6	86.4	78.2				
1	0	10	44.5	42.7	3	162.7	161.2	8	48.9	48.9	5	59.9	59.5	5	51.6	52.4						
7			107.2	99.0	6	138.1	134.9	14	36.1	40.2	12	61.4	52.8	0	94.4	79.1						
4			48.5	55.6	12	4.7*	25.7	12	1	14	4.8*	17.8	3	151.7	127.6	4	51.3	53.3				
15			81.4	68.1	15	5.0*	26.7	9	70.5	66.7	6	54.5	51.0	7	31.0	34.5						
14	1	10	38.5	37.7	11	1	12	10.6*	37.5	6	91.6	60.9	9	112.4	104.5	11	23.5*	20.5				
11			50.3	56.7	10	20.1*	29.4	3	60.3	61.6	12	152.6	135.3	11	5	18	55.2	54.2				
8			89.1	69.7	7	3.6*	10.2	0	168.0	164.0	10	3	16	4.7*	21.0	8	64.5	63.8				
5			41.0	40.7	4	53.1	39.6	1	2	14	60.4	60.1	7	44.3	46.9	5	62.3	63.7				
2			177.7	172.5	1	91.8	25.6	4	126.9	130.6	4	108.9	104.9	2	122.3	123.7						
0	2	10	128.0	327.3	2	2	12	239.0	230.8	7	58.6	56.7	1	115.3	115.2	0	6	18	159.4	142.0		
3			67.6	59.6	5	172.6	169.6	10	63.6	57.3	2	4	125.7	122.4	3	27.6	35.7					
6			66.4	66.2	8	68.1	58.5	13	4.9*	13.3	5	101.1	101.0	6	4.6*	30.5						
9			53.1	51.2	11	66.6	68.3	11	3	14	41.7	48.7	8	4.5*	25.3	9	4.9*	27.3				
12			25.1*	35.4	8	53.6	51.0	11	11	42.6	45.7	7	7	18	66.6	63.6						
13	3	10	37.7	37.9	12	3	12	4.8*	7.1	5	49.1	51.8	9	5	16	40.7	40.9	4	58.7	57.8		
10			25.3*	18.7	9	44.6	46.0	6	138.7	133.7	6	73.9	72.2	1	68.9	67.1						
7			89.1	69.7	7	26.9	37.1	0	4	14	127.8	128.7	3	17.4*	15.3	2	8	18	4.5*	20.2		
4			202.6	203.4	3	44.2	24.4	3	58.1	61.2	0	151.0	152.7	5	31.5	32.7						
1			95.7	88.4	0	147.1	145.3	6	50.1	50.3	1	6	52.9	54.4	8	4.9*	15.2					
2	4	10	86.2	84.9	1	4	12	128.7	126.7	9	57.8	63.1	4	35.5	37.2	6	9	18	27.5	41.1		
5			80.3	82.3	4	101.7	97.4	12	12.7*	32.7	7	5.4*	34.5	3	64.5	68.2						
8			32.5	39.2	7	114.5	108.0	10	5	14	4.9*	22.2	10	4.8*	6.5	0	126.2	130.4				
11			7.7*	33.8	10	4.6*	4.2	6	63.5	65.7	8	7	16	23.0*	33.9	1	10	18	4.5*	17.3		
12	5	10	14.9	12.6	11	5	12	49.0	47.4	4	125.4	127.1	5	9.5*	32.8	4	4.8*	14.8				
9			68.5	66.0	0	21.4*	27.9	1	40.3	40.5	2	66.7	66.4	5	51.1	51.1						
6			64.4	64.5	5	77.4	69.7	2	6	14	27.5	36.8	0	32.5	41.8	2	48.8	51.2				
3			36.0	33.6	2	108.9	105.7	5	62.4	60.0	3	57.9	60.6	0	0	12	32.3	29.9				
0			126.0	122.0	0	6	12	195.7	202.0	8	57.5	59.5	6	4.7*	19.5	3	4.7*	11.8				
1	6	10	61.9	61.4	3	98.7	100.8	7	67.2	67.9	7	9	16	51.4	60.4	1	13	18	5.4*	37.4		
4			12.1*	18.5	6	43.2	31.7	6	60.9	67.9	4	50.8	60.5	2	13	19	4.9*	8.1				
7			17.1*	23.5	9	4.8*	30.2	3	71.1	55.5	1	4.9*	17.3	1	12	12	4.9*	6.8				
10			29.1*	29.3	10	4.9*	4.9	4	187.8	192.5	2	10	16	42.9	49.3	3	11	19	4.7*	13.6		
8	7	10	21.4*	25.0	7	41.9	52.3	1	18	14	15.6*	29.1	5	28.9*	32.7	5	10	19	4.9*	14.1		
5			84.7	86.3	4	92.4	91.6	4	4.5*	12.2	3	31.1	32.9	40.0	2	4.6*	17.0					
2			124.3	131.4	1	49.9	55.6	7	24.3*	25.7	0	91.2	89.9	1	9	19	4.5*	12.9				
0	8	10	42.5	47.9	2	8	12	79.1	77.7	9	8	9.4*	10.3	1	12	16	4.7*	5.1	4.7*	1.6		
3			24.9*	31.8	5	36.9	45.3	5	64.1	66.2	4	46.8	38.2	7	4.9*	6.1						
6			8.6*	12.4	2	5.0*	16.7	2	77.4	84.0	2	13	16	44.3	49.0	6	8	19	4.7*	4.6		
9			50.7	23.2	6	9.1*	35.5	5	59.6	32.7	1	11	17	4.8*	18.6	2	7	19	16.9*	26.9		
4			51.6*	51.8	5	87.5	38.7	6	4.9*	16.6	2	12	17	4.8*	13.4	5	4.5*	4.8				
1			35.5	55.1	1	10	12	4.5*	29.9	4	41.1	40.0	11	17.2*	20.6	8	4.8*	10.1				
2	10	10	26.6	23.6	4	50.9	45.5	1	24.0*	21.3	4	4.9*	11.5	11	6	19	4.9*	51.9				
5			22.6*	27.1	7	5.9*	23.0	2	12	14	6.9*	24.2	6	10.7	13.5	7	4.7*	3.5				
6	11	10	6.8*	18.3	5	11	32.9	39.9	3	13	14	42.4	45.1	3	16.4*	20.8	4	4.2*	13.9			
3			59.8	51.1	2	34.7	34.5	0	69.7	63.9	2	9	17	4.4*	18.3	1	3.8*	9.8				
0			115.6	108.8	0	12	60.2	61.0	1	14.4	14.8*	16.3	5	5.7*	3.7	3	5	19	3.8*	2.3		
1	12	10	24.7*	34.8	5	4.9*	3.2	2	8	15	4.8*	5.5	7	8	17	4.9*	12.2	6	4.5*	12.9		
4			4.7*	20.0	5	10	13	12.5*	51.0	8	15	4.9*	12.9	4	4.4*	9.7	9	4.7*	4.1			
3			4.8*	17.7	1	9	13	4.1*	22.3	2	4.1*	12.6	7	4.4*	11.3	9	4.4*	11.2				
2	9	11	23.9*	36.4	4	4.5*	7.9	1	7	15	3.7*	6.5	10	19.1*	11.9	8	4.5*	8.9				
5			4.7*	9.3	9	4.8*	9.4	9	4.2*	18.4	4	4.5*	5.6	5	4.5*	36.8						
8			4.8*	5.6	9	8	13	4.7*	6.9	7	4.7*	8.6	9	4.4*	0.8	2	16.0	20.0				
7	8	11	14.7*	14.5	10	4.5*	11.4	10														

Table 3B. (Continued)

h	k	l	F_o	F_c	h	k	l	F_o	F_c	h	k	l	F_o	F_c	h	k	l	F_o	F_c					
10	2	20	4.7*	8.5	5	7	22	66.6	61.6	3	5	25	22.9*	5.4	10	3	28	5.0*	33.6					
11	3	20	25.8*	29.1	2	8	22	59.2	61.5	2	17	17.3	28.0*	35.1	5	4.4*	18.5	4.4*	18.5					
8		30.1	37.1	0	8	22	55.1	50.1	9	16.8*	11.5	4	64.1	67.0	8	4.7*	14.0	4.7*	14.0					
5		23.2*	10.7	3			27.3*	29.6	8	4	25	4.8*	12.6	1	36.1	39.9	10	0	31	4.6*	0.0			
2		116.7	116.0	6			4.9*	24.1	5	4.5*	12.8	2	4	28	70.5	74.8	7	4.6*	0.0	4.6*	0.0			
0	4	20	115.5	112.9	4	9	22	68.9	67.8	2	4.0*	21.9	45.3	50.6	4	4.5*	0.0	4.5*	0.0	4.5*	0.0			
3		91.2	94.5	1			20.5*	28.6	1	3	25	27.8	26.9	8	4.9*	11.5	1	4.1*	0.0	4.1*	0.0			
6		52.2	34.8	2	10	22	4.7*	18.0	4	4.1*	17.7	6	5	28	50.5	56.3	2	0	32	75.6	74.9			
9		64.1	61.2	5			4.8*	12.4	7	4.5*	11.1	3	4.5*	14.4	5	65.9	71.7							
10	5	20	4.9*	21.2	3	11	22	47.7	45.9	10	10.1*	14.8	0	110.3	112.9	8	4.4*	24.1	4.4*	24.1				
7		11.7*	34.1	0			44.6	50.9	9	2	25	4.8*	21.8	1	6	28	4.0*	20.0	9	1	32	20.1*	25.6	
4		96.5	90.9	1	12	22	4.9*	11.1	6	4.5*	13.3	4	26.0*	23.5	6	57.5	62.9							
1		48.6	47.3	2	12	23	4.9*	2.3	3	20.2*	38.1	7	35.8	37.7	3	55.1	51.6							
2	6	20	58.2	34.1	1	12	23	4.9*	4.1	2	125	14.6*	31.5	5	7	28	22.4*	27.5	0	0	32	54.5	63.6	
5		79.1	6.6	3	10	23	4.9*	8.2	2	4.0*	11.2	2	4.0*	17.3	1	2	32	14.7*	23.2					
9		1.2*	10.4	2	9	23	4.7*	14.4	8	15.6*	16.4	2	8	28	46.7	65.9	4	4.5*	16.2	4.5*	16.2			
9	7	20	47.8	54.7	5			5.0*	7.1	3	4.8*	15.7	7	7	65.0	57.3								
6		6.7*	20.2	7	8	23	4.9*	4.1	10	0	25	4.7*	0.0	6	5.7*	14.0	8	3	32	31.0*	41.1			
3		26.6*	34.6	4			4.7*	8.8	7	4.5*	0.0	4	9	28	59.6	63.6	5	16.4*	32.6					
0		76.5	76.5	1			4.4*	24.0	4	3.9*	0.0	1	4.7*	13.9	2	69.1	69.5							
1	8	20	37.2	34.6	3	7	23	4.4*	11.7	1	3.5*	0.0	2	10	28	9.5*	22.4	0	4	32	90.9	88.1		
4		1.8*	30.6	6			4.7*	7.0	2	0	26	147.4	142.3	0	11	28	39.6	46.6	3	28.6	51.2			
7		43.5	46.6	8	6	23	4.9*	2.6	5	53.0	54.7	1	11	29	4.7*	10.6	6	4.8*	13.6					
5	9	20	29.2*	36.7	5			4.5*	10.1	8	9.9*	30.7	10	3	29	10.0*	7.7	7	5	32	9.2*	24.2		
2		87.7	88.6	2			11.7*	26.7	11	70.2	65.7	2	2	29	4.7*	8.2	4	59.2	55.7					
0	10	20	38.0	41.7	1	5	23	15.2*	33.2	12	1	26	38.5	35.4	4	8.8*	2.1	1	42.4	46.8				
3		4.8*	21.1	4			2.0*	15.7	9	4.1*	11.4	1	4.1*	18.7	2	6	32	21.4*	38.9					
6		24.5*	20.7	7			4.7*	11.1	6	50.8	30.6	6	7	29	4.7*	9.8	5	16.4*	25.5					
4	11	20	24.5*	39.7	10		15.0*	28.9	3	2.3*	17.4	2	4.7*	13.8	3	7	32	4.4*	23.6					
1		33.9	38.1	9	4	23	4.8*	5.0	0	28.6	29.3	5	6	29	4.8*	21.5	0	67.2	73.7					
2	12	20	52.4	48.3	6		4.5*	16.4	4	3.7*	1.8	2	4.5*	11.3	1	8	32	4.7*	18.0					
0	13	20	42.5	41.4	3		24.1*	41.5	4	4.0*	40.7	4	5.5*	13.4	4	20.4*	20.0							
1	13	21	4.8*	9.0	2	3	23	22.0*	25.6	7	61.2	57.0	4	4.8*	16.8	2	9	32	66.9	65.7				
3	12	21	10.6*	5.4	5		4.1*	12.7	10	4.9*	26.1	7	4.7*	12.6	0	10	32	29.8*	40.7					
2	11	21	11.4*	9.0	8		4.6*	17.1	8	3	26	12.3*	17.4	9	4.8*	10.1	2	8	33	4.8*	25.2			
4	10	21	4.8*	5.7	11		4.8*	9.2	2	26	28.7	33.6	6	4.7*	14.5	1	7	33	4.7*	4.2				
1		4.6*	15.1	10	2	23	4.8*	1.9	2	37.1	49.6	5	4.5*	12.6	4	4.8*	9.6							
3	9	21	4.1*	11.4	7		4.5*	11.4	0	4	26	134.5	170.0	2	3	29	4.2*	1.8	6	6	33	4.8*	6.5	
6		4.8*	9.6	4			3.6*	13.3	3	4.8*	9.8	9	4.8*	88.8	5	10	4.8*	18.8	3	6.6*	12.2			
5	8	21	4.7*	3.6	1		5.9*	27.0	6	5.0*	27.3	8	4.8*	15.1	2	5	33	4.7*	8.7					
2		22.7*	36.2	3	1	23	15.2*	30.9	9	5.0*	27.3	10	2	29	4.9*	4.2	5	4.8*	12.7	4.8*	12.7			
1	7	21	30.4	30.5	6		4.1*	13.8	7	5	26	54.5	55.2	7	4.6*	13.9	2	4	33	4.8*	10.8			
4		6.4*	16.5	9			4.7*	12.3	4	4.1*	41.9	46.8	4	4.5*	8.1	1	51.0	51.6						
7		4.7*	1.2	12			4.8*	5.7	1	15.1*	23.2	1	4.7*	7.2	3	5	33	18.2*	25.5					
9	6	21	4.9*	8.9	11	0	23	4.8*	0.0	2	6	26	49.4	46.2	3	1	29	4.1*	7.2	6	4.8*	14.9		
6		28.0	14.4	8			4.5*	0.0	5	21.8*	26.3	6	4.5*	14.1	6	4.8*	15.2	8	2	33	4.8*	15.2		
3		21.2*	27.9	5			5.8*	0.0	8	4.9*	9.3	9	4.7*	16.2	4	4.6*	15.9							
2	5	21	3.9*	13.7	2		3.5*	0.0	6	7	26	25.5*	38.4	11	0	29	4.9*	0.0	5	30.4	25.9			
5		4.5*	7.7	0	0	24	100.8	97.3	3	65.4	59.9	8	4.7*	0.0	2	7	34	4.7*	0.0	1	1	33	4.5*	11.0
8		11.5*	10.2	3			79.6	79.0	0	76.8	82.6	5	4.7*	0.0	4	4.0*	0.0	4	4.5*	17.2				
10	4	21	4.8*	15.5	6		84.6	80.9	1	8	26	27.7*	27.5	2	4.0*	0.0	4	4.5*	22.8					
7		4.5*	15.2	9			67.1	66.2	4	4.1*	2.0	52.2	52.6	3	18.4*	34.6	9	0	33	4.4*	0.0			
1		22.5*	20.2	12			42.2	43.1	5	5.9	26.5	33.0	6	62.3	61.9	4	4.7*	0.0						
1		26.4	30.3	10	1	24	4.8*	18.2	2	33.8	37.0	6	6.7*	13.6	48.3	68.3	3	6.7*	0.0					
3	3	21	11.4*	29.6	7		28.6	37.7	0	10	26	6.7*	13.6	9	3	30	19.5*	65.2	0	2	34	66.4	64.5	
6		4.2*	11.8	4			80.6	78.5	3	4.7*	4.0	10	1	50	4.9*	13.9	1	0	34	37.3	35.2			
9		17.2*	17.1	1			88.3	78.0	1	11	26	31.5	36.0	7	6.1*	28.9	4	61.4	58.1					
12		4.9*	10.9	2	1	24	88.7	90.6	10	2	11	27	4.8*	1.1	41.4	37.7	7	33.2	38.1					
11	2	21	4.8*	11.5	5		99.2	96.1	1	10	27	4.8*	6.1	1	10.5*	34.4	10	4	4.8*	4.4				
8		4.4*	8.7	3	24		4.6*	19.7	3	9	27	4.8*	18.5	18.5	2	50	92.7	92.0	8	1	34	18.8*	7.4	
5		3.9*	16.1	11			44.5	41.7	5	4.8*	10.1	5	7.9	76.7	5	4.6*	7.7							
2		6.4*	8.7	9	3	24	16.8*	35.5	5	19.6*	33.1	8	21.9*	8.4	2	21.2*	40.1							
1	1	21	21.5	17.8	6		81.6	79.3	1	7	27	4.4*	6.9	9	3	30	18.5*	65.2	0	2	34	66.4	65.5	
4		25.7*	29.5	3			41.6*	41.4	4	4.7*	8.0	6	49.4	44.7	3	6.4*	34.7							
7		18.1*	17.0	0			4.8*	83.7	4	4.7*	0.7	3	4.4*	92.1	7	3	3							

Table 5. Distances(Å) for boron and oxygen atoms in boracite*

Atoms	B(1)-1	B(1)-2	B(1)-3	B(2)-1	B(2)-2	B(2)-3	B(3)
O(1)				R 1.581 (7)	R 1.555 (7) R 1.437 (6)	R 1.543 (5)	[2.303 (5)]
O(2)-1	R 1.461 (6)						
O(2)-2			R 1.463 (7)	R 1.455 (6)			
O(2)-3		R 1.468 (7)			R 1.464 (8)		
O(2)-4			1.455 (7)	1.449 (7)			
O(2)-5	1.476 (7)				1.454 (6)		
O(2)-6		R 1.460 (8)		R 1.440 (8)			
O(2)-7		1.493 (6)					1.375 (6)
O(2)-8	1.510 (7)						1.382 (6)
O(2)-9	R 1.462 (6)					R 1.461 (5)	
O(2)-10		1.473 (6)	R 1.453 (7)			1.452 (6)	
O(2)-11			1.509 (7)			R 1.447 (6)	
O(2)-12							1.369 (6)
averages	<u>1.477</u>	<u>1.474</u>	<u>1.470</u>	<u>1.481</u>	<u>1.478</u>	<u>1.476</u>	<u>1.375</u>
B(1)-1					R 2.450 (8) 2.518 (8)	R 2.451 (7)	2.475 (8)
B(1)-2				R 2.460 (10)	R 2.469 (9)	2.529 (7)	2.453 (7)
B(1)-3				R 2.469 (8) 2.517 (8)		R 2.459 (8)	2.472 (8)
B(2)-1					R 2.628 (5)	R 2.623 (8)	[3.097 (8)]
B(2)-2						R 2.596 (8)	[3.083 (8)]
B(2)-3							[3.080 (6)]

averages: B(1)-B(2) sets, 6 R 2.460; B(2)-B(2) set, 3 R 2.616; 6 nonring B-B 2.494.

average O—O, tetrahedra: all (36) 2.410; O(1) only (9) 2.448.

triangle (3) 2.375.

* Error in parentheses is one standard deviation; for 1.461(6) read $1.461 \pm 0.006 \text{ \AA}$, etc.; R refers to the distances within a ring (see Fig. 1).

Table 6. Angles of the borate framework in boracite

Central atom	Other atoms*	B—O—B ring angles**
O(1)	B(2)-1, B(2)-2	113.8 (3)°
	B(2)-1, B(2)-3	114.2 (4)
	B(2)-2, B(2)-3	113.9 (4)
O(2)-1	B(1)-1, B(2)-2	115.4 (4)
O(2)-2	B(1)-3, B(2)-1	115.6 (5)
O(2)-3	B(1)-2, B(2)-2	114.8 (4)
O(2)-6	B(1)-2, B(2)-1	116.0 (3)
O(2)-9	B(1)-1, B(2)-3	114.0 (4)
O(2)-9	B(1)-1, B(2)-3	114.0 (4)
O(2)-11	B(1)-3, B(2)-3	116.0 (4)
	average (9)	114.9°

Central atom	Other atoms*	O—B—O ring angles**
B(1)-1	1, 9	112.5 (4)°
B(1)-2	3, 6	112.1 (4)
B(1)-3	2, 11	112.0 (4)
B(2)-1	2, O(1)	106.6 (3)
	6, O(1)	108.4 (4)
B(2)-2	1, O(1)	109.3 (4)
	3, O(1)	107.3 (4)
B(2)-3	9, O(1)	107.6 (4)
	11, O(1)	109.3 (4)
	average (9)	109.5°

Central atom	Other atoms*	B—O—B cross-linking angles
O(2)-4	B(1)-3, B(2)-1	120.1 (4)°
O(2)-5	B(1)-1, B(2)-2	118.5 (4)
O(2)-7	B(1)-2, B(3)	117.6 (4)
O(2)-8	B(1)-1, B(3)	117.6 (4)
O(2)-10	B(1)-2, B(2)-3	119.6 (4)
O(2)-12	B(1)-3, B(3)	118.3 (4)
	average (6)	118.6°

(Table 6. (*Continued*)

Central atom	Other atoms*	O—B—O angles, triangle
B(3)	7, 8	119.0 (4)
	7, 12	119.6 (4)
	8, 12	119.7 (4) $\Sigma = 358.3^\circ$

[Nonplanar, see Table 8]

Central atom	Other atoms*	O—B—O angles, tetrahedra non-ring
B(1)-1	1, 5	108.6 (4)°
	1, 8	107.5 (4)
	5, 8	112.3 (4)
	5, 9	109.6 (4)
	8, 9	106.4 (4)
B(1)-2	3, 7	107.7 (3)
	3, 10	107.7 (5)
	6, 7	107.7 (5)
	6, 10	108.5 (3)
	7, 10	113.2 (4)
B(1)-3	2, 4	109.2 (5)
	2, 12	106.0 (4)
	4, 11	109.6 (4)
	4, 12	112.6 (4)
	11, 12	107.4 (5)
B(2)-1	2, 4	109.3 (4)
	2, 6	111.1 (5)
	4, 6	111.4 (4)
	4, O(1)	109.8 (5)
B(2)-2	1, 3	109.9 (4)
	1, 5	110.3 (4)
	3, 5	110.0 (5)
	5, O(1)	108.3 (2)
B(2)-3	9, 10	109.4 (4)
	9, 11	111.2 (3)
	10, 11	109.0 (4)
	10, O(1)	110.5 (3)
	overall average (27)	109.4°

* Where numbers only are given, the atom is an O(2) type.

** Error in parentheses is one standard deviation; for 113.8 (3) read
113.8 \pm 0.3°, etc.

Table 7. Comparison of average B—O values for borates having one oxygen atom linked to three tetrahedral boron atoms

Compound	Reference	Average B—O distance		
		Tetrahedra		Triangle
		for O to three B	for all other O	
Macallisterite, $\text{Mg}_2[\text{B}_6\text{O}_7(\text{OH})_6]_2 \cdot 9\text{H}_2\text{O}$	DAL NEGRO <i>et al.</i> (1969)	1.528 Å	1.458 Å	1.364 Å
Aksaite, $\text{MgB}_6\text{O}_7(\text{OH})_6 \cdot 2\text{H}_2\text{O}$	DAL NEGRO <i>et al.</i> (1971)	1.518	1.453	1.365
Tunellite, $\text{SrB}_6\text{O}_9(\text{OH})_2 \cdot 3\text{H}_2\text{O}$	CLARK (1964)	1.51	1.46	1.36
Strontioginorite, $\text{SrCaB}_{14}\text{O}_{20}(\text{OH})_6 \cdot 5\text{H}_2\text{O}$	KONNERT <i>et al.</i> (1970)	1.52	1.45	1.37
B_2O_3 II	PREWITT and SHANNON (1968)	1.508	1.373	none
$\text{SrO} \cdot 2\text{B}_2\text{O}_3$	PERLOFF and BLOCK (1966)	1.550	1.438	none
Boracite, $\text{Mg}_3\text{ClB}_7\text{O}_{13}$	This paper	1.559	1.464	1.375

tetrahedra and a triangle. The deviations of the ring boron atoms from the plane defined by the three ring oxygen atoms are given in Table 8 and are appreciable for two of the boron atoms in each ring (± 0.7 – 0.8 Å). Although the distances and angles of the cross-linking triangle are normal (Tables 5 and 6), the B(3) atom does lie about 0.1 Å out of the plane of the three associated oxygen atoms. To this slight extent it approaches “pyramidal” more than do most boron-oxygen triangles recorded to date, for which exact planarity of all four atoms is normally found within the limits of accuracy.

Coordination of metal and chlorine ions

The coordination of the (Mg,Fe) cations in orthorhombic boracite and its iron-rich analogue is fivefold and is probably best described as transitional between square pyramidal and trigonal bipyramidal. (These are the two common types of five-coordination: *e.g.* GILLESPIE, 1963; COTTON and WILKINSON, 1966, p. 410 ff.). Four oxygen anions

Table 8. *Boroxol rings in boracite and deviations from planarity**

Plane	Oxygen atoms defining ring or triangle	Boron atoms	Distance of boron atoms from plane of oxygen atoms	Angles between planes of oxygen atoms
1	O(1), O(2)-1, O(2)-9	B(1)-1	- 0.05 Å	1, 2 73°
		B(2)-2	- 0.70	1, 3 73
		B(2)-3	+ 0.78	
2	O(1), O(2)-2, O(2)-11	B(1)-3	+ 0.06	2, 3 73
		B(2)-1	- 0.74	
		B(2)-3	+ 0.65	
3	O(1), O(2)-3, O(2)-6	B(1)-2	+ 0.08	
		B(2)-1	+ 0.65	
		B(2)-2	- 0.75	
4	O(2)-7, O(2)-8, O(2)-12	B(3)	+ 0.11	

* Plane of oxygen atoms (see Fig. 1).

Table 9. *Distances for the Mg and Cl coordination in boracite, (Fe,Mg) and Cl in the iron-rich analogue*

(Mg,Fe) atom	Coordinating atoms*		Distance**	
	Boracite	Iron-rich analogue	Boracite	Iron-rich analogue
(Mg,Fe) (1)	9	3	2.010 (4) Å	2.049 (7) Å
	12	2	2.050 (4)	2.092 (9)
	1	1	2.059 (4)	2.066 (5)
	4	4	2.064 (4)	2.113 (9)
	average (4)		2.046	2.080
		Cl	2.616 (2)	2.567 (3)
		[Cl']	3.447 (2)	3.536 (3)
Oxygen atoms in base				
	1-12	1-2	2.845 (5)	2.90 (1)
	1-9	1-4	2.850 (5)	2.88 (1)
	4-12	3-2	2.869 (5)	2.89 (1)
	4-9	3-4	2.973 (4)	3.05 (1)
	average (4)		2.884	2.93

Table 9. (Continued)

Mg atom	Coordinating atoms*	Distance**		Mg atom	Coordinating atoms*	Distance**	
		Boracite	Boracite			Boracite	Boracite
Mg(2)	3	2.023 (4) Å		Mg(3)	2	2.013 (4) Å	
	10	2.035 (4)			11	2.022 (5)	
	8	2.056 (5)			6	2.038 (4)	
	5	2.060 (4)			7	2.062 (4)	
	average	<u>2.044</u>				<u>2.034</u>	
	Cl	2.614 (2)			Cl	2.615 (2)	
	[Cl']	3.443 (2)			[Cl']	3.430 (2)]	
Oxygen atoms in base				Oxygen atoms in base			
	3-8	2.787 (6)			2-7	2.843 (5)	
	8-10	2.842 (4)			7-11	2.857 (4)	
	3-5	2.932 (4)			6-11	2.906 (5)	
	5-10	2.980 (6)			2-6	2.907 (4)	
	average	<u>2.885</u>				<u>2.878</u>	
Mg atom number	Oxygen atoms defining plane***		Distance in boracite of				
	Boracite		oxygen atoms from plane***	Mg cations from plane***			
Mg(1)	1, 4, 9, 12		± 0.27 Å	— 0.30 Å			
Mg(2)	3, 5, 8, 10		± 0.26	— 0.27			
Mg(3)	2, 6, 7, 11		± 0.29	— 0.27			

* Numbers are those of O(2) atoms.

** Error in parentheses is one standard deviation; for 2.010 (4) read 2.010 ± 0.004 Å, etc.

*** Best least-squares plane.

form a rectangular approximation to a "square" base, and the chlorine ion serves as the apex (Fig. 3). However, the four basal oxygen atoms do not lie in exactly the same plane (Table 9); two are approximately collinear with the (Mg,Fe) cation and perpendicular to the apical chlorine ion, but the other two are below the perpendicular. Considering the angles involved, two oxygen atoms and a chlorine ion can be taken as the waist atoms of a trigonal bipyramidal, with the other oxygen

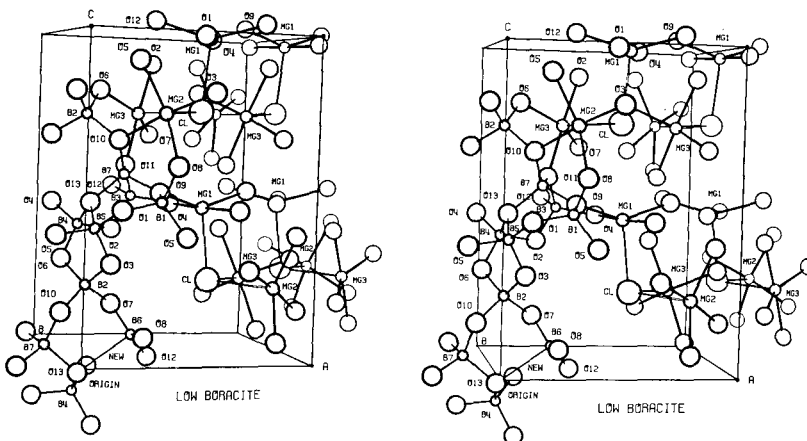


Fig. 3. Stereoscopic-pair view of a selected portion of the orthorhombic boracite structure, showing the coordination for Mg cations and the Cl anion. Atom labelling as in Fig. 2. Drawing produced by ORTEP (JOHNSON, 1965)

atoms at the vertices. Mg(1) in boracite can be taken as an example: as given in Table 10, O(12)—Mg—Cl 101.2°, O(9)—Mg—Cl 111.4°, and O(9)—Mg—O(12) 147.1° can be considered transitional between the ideal 90° angle of a square pyramidal array and the ideal 120° angle for the waist points of a trigonal bipyramidal. Taking the other two oxygen atoms [all O(2) type], O(1) and O(4), to the "waist" atoms, we find a range from 87.6° to 93.7° with an average 90.1°, close to the expected 90°. Between the two apices we have O(1)—Mg—O(4) 175.9° instead of the ideal 180°. Similar values are found for Mg(2) and Mg(3), as well as for the (Fe,Mg) atom in the iron-rich analogue.

A somewhat similar coordination was found by CODA *et al.* (1967) for two of the four distinct, five-coordinated Mg atoms in the crystal structure of wagnerite, Mg_2PO_4F , where fluorine atoms take the place of the chlorine atoms in boracite. The Mg(5) and Mg(7) atoms in wagnerite have a range of angles from 104° to 136° in the waists of the trigonal bipyramids, and the other two five-coordinated Mg atoms in wagnerite, Mg(1) and Mg(3), have a close approximation to ideal trigonal bipyramidal as the angles around the waists deviate from the ideal 120° value by only $\pm 8^\circ$. Thus we find in these two structures, boracite and wagnerite, coordination transitional between square pyramidal and trigonal bipyramidal, illustrated by the sequence: boracite and its iron-rich analogue, wagnerite Mg(5) and Mg(7), and wagnerite Mg(1) and Mg(3).

In general the ideal value of 120° would be expected only if all coordinating atoms were of the same species. In the cases of boracite and wagnerite, the inclusion of one large halogen atom in the three ligands which form the waist of the trigonal bipyramidal probably tends to make the ideal halogen-cation-oxygen angle slightly greater than 120° , perhaps ideally close to the 125° to 128° values found for one angle each of the wagnerite Mg(1) and Mg(3) sites. Considerations of this sort may also explain why the halogen atom is one of the ligands about the waist of the "trigonal bipyramidal", rather than taking the more symmetrical and aesthetically pleasing position as one of the apical ligands. Assuming mutual contact of the waist ligands, the presence of the larger halogen atom allows a slightly larger hole to be formed, and this may be helpful in accomodating the Mg^{2+} ion.

In the boracite-like structures, we suggest that the five-coordination, which is rare for iron and magnesium, is due more to the nature of the cavities available than to requirements of spatially directed bonding. This suggestion follows an observation by WELLS (1962, p. 869) in connection with anomalous behavior of Cu^{2+} in organic complexes. It would also explain why the five-coordination is a compromise between square pyramidal and trigonal bipyramidal, even though the latter is generally more favorable energetically for isolated molecules (GILLESPIE, 1963).

The cation-oxygen distances are normal (Table 9). The average Mg—O distance of 2.041 \AA in boracite compares well with the average of 2.042 \AA for the five coordinating oxygen atoms in grandidierite (STEPHENSON and MOORE, 1968), and the average of 2.038 \AA for the four coordinating oxygen atoms in wagnerite (CODA *et al.*, 1967)³. There seem to be no accurately refined structures with iron in five-coordination, but the average cation-oxygen distance of 2.080 \AA in the iron-rich analogue of boracite is about as much larger than that of boracite as would be predicted from the sums of ionic radii (SHANNON and PREWITT, 1969, 1970). The cation-chlorine distances, however, seem to be anomalous. The average cation-chlorine distance is 2.615 \AA in boracite, but only 2.567 \AA in the trigonal form, despite the presence of the larger iron ion. Again, this apparent anomaly may be due to the configuration of the cavities, in conjunction with subtle differences between the orthorhombic and trigonal structures. The principal alter-

³ Yoderite (FLEET and MEGAW, 1962) contains magnesium in five-coordination with oxygen, but the site also has aluminum so that the bond distances are not readily comparable.

native explanation would invoke an effect of bonding properties or electronic structure, but crystal-field theory, which one would assume to be applicable in this case, does not provide an explanation for the anomaly. DORMANN (1970) has described the $3z^2-r^2$ orbital as being the lowest in energy in Ni^{2+} equivalents of boracite. If this is true also for Fe^{2+} , this orbital, which is directed toward the chlorine ion, should be occupied by the sixth d electron of the ferrous iron and tend to cause a *longer* cation-chlorine distance than expected. Actually it is the Mg—Cl distance in boracite which is anomalously long. A theoretical distance of 2.48 Å may be computed from the ionic radii of Cl^{1-} in sixfold coordination (SHANNON and PREWITT, 1969) and Mg^{2+} in five-fold coordination (SHANNON and PREWITT, 1970). This is far less than the observed 2.615 Å. If we add 0.05 Å, the difference between the ionic radii of Mg^{2+} and Fe^{2+} (in sixfold coordination, SHANNON and PREWITT, 1969), to the predicted distance, we come close to the observed (Fe,Mg)—Cl distance in the trigonal form, 2.567 Å. The observed (Fe,Mg)—Cl distance is still slightly longer than predicted, even considering that about twenty percent of this site is occupied by magnesium, but some lengthening would be expected from the fact that the chlorine ion is in threefold, rather than sixfold coordination, as well as from charge-balance considerations discussed below.

In the cubic form as described by ITO *et al.* (1951), the chlorine anion has a perfect octahedral arrangement of Mg or Fe cations around it at a distance of about 3 Å, and the cations are also coordinated in an octahedral fashion with the two apical chlorine anions at equal distances. In the orthorhombic and trigonal structures three of the cations are removed to distances of about 3.45 Å in boracite, 3.54 Å in the analogue; the Cl—(Fe,Mg)—Cl angles are 171.6° to 176.2°. The shifts of the cation and halogen atoms between their positions in the cubic and lower symmetry forms, which together with the shifts of the B(3) and O(1) atoms account for the polarity of the lower symmetry forms, have been discussed by SCHMID (1970), for example, and in our previous note (DOWTY and CLARK, 1972 b).

On the basis of idealized atomic shifts from the high-temperature structure, SCHMID and TROOSTER (1967) assumed that there would be two distinct types of metal coordination in orthorhombic boracite structures, with Mg(1) being of one type and Mg(2), Mg(3) of the other. This assumption appeared to be confirmed by their Mössbauer spectra of synthetic trigonal, orthorhombic, and cubic forms of $\text{Fe}_3\text{ClB}_7\text{O}_{13}$; the trigonal and cubic forms each showed only one ferrous doublet, but the

orthorhombic form showed two very distinct doublets with an area ratio of approximately two to one. The doublet with the smaller area in the orthorhombic form appeared to be identical to the single doublet in the trigonal form.

A comparison of the bond angles of the cation coordinations (Table 10) in the orthorhombic and trigonal forms shows that for many of the angles there is slightly greater similarity of the (Fe,Mg) coordination in the trigonal form with Mg(1) of the orthorhombic form than with Mg(2) and Mg(3). However, the differences between Mg(1) and the other two are minor, as large as three degrees for only three of the angles, and the differences between Mg(2) and Mg(3) are in some cases practically as large. The bond distances (Table 9) allow no significant distinction to be made among the three magnesium atoms. Evidently the atomic shifts of the Mg and Cl atoms are not as ideal as thought, and oxygen atoms also shift slightly in adjustment, so that

Table 10. Angles for the Mg,Cl coordination on boracite and the (Fe,Mg),Cl coordination in the iron-rich analogue

(Mg,Fe) atom	Atoms of O—Mg—O,Cl angle*		Angle**	
	Boracite	Iron-rich analogue	Boracite	Iron-rich analogue
1	1, 12	1, 4	87.6 (1)°	87.1 (3)°
	4, 12	1, 2	88.4 (2)	88.4 (3)
	1, 9	2, 3	88.9 (2)	88.6 (3)
	4, 9	3, 4	93.7 (1)	94.3 (3)
	9, 12	1, 3	147.1 (2)	146.0 (2)
	1, 4	2, 4	175.9 (2)	175.3 (2)
	1, Cl	4, Cl	88.4 (2)	90.2 (1)
	4, Cl	2, Cl	93.5 (2)	92.7 (1)
	12, Cl	3, Cl	101.2 (1)	102.1 (1)
	9, Cl	1, Cl	111.4 (1)	111.8 (2)
Atoms of O—O—O angles around base				
	9-4-12	1-4-3	83.6 (1)	83.2 (3)
	9-1-12	1-2-3	86.2 (1)	85.7 (3)
	1-9-4	2-3-4	90.0 (1)	89.7 (3)
	4-12-1	2-1-4	92.3 (1)	93.2 (3)
	average (4)		88.0	88.0

Table 10. (*Continued*)

Mg atom	Atoms of O—Mg—O, Cl angle*	Angle**	Mg atom	Atoms of O—Mg—O, Cl angle*	Angle**
	Boracite	Boracite		Boracite	Boracite
2	3, 8	86.2 (2)°	3	2, 7	88.5 (2)°
	8, 10	88.0 (2)		7, 11	88.8 (2)
	3, 5	91.8 (2)		6, 11	91.4 (2)
	5, 10	93.4 (2)		2, 6	91.7 (2)
	5, 8	150.7 (2)		6, 7	148.9 (2)
	3, 10	174.2 (2)		2, 11	176.9 (2)
	3, Cl	90.2 (1)		2, Cl	86.9 (1)
	10, Cl	91.4 (1)		11, Cl	92.5 (1)
	5, Cl	100.6 (2)		6, Cl	102.4 (1)
	8, Cl	108.7 (1)		7, Cl	108.7 (1)
Atoms of O—O—O angles around base			Atoms of O—O—O angles around base		
5-10-8		86.3 (1)	6-11-7		86.5 (1)
3-5-10		86.6 (1)	7-2-6		86.8 (1)
8-3-5		88.2 (1)	2-6-11		87.9 (1)
10-8-3		82.1 (2)	11-7-2		90.1 (1)
average (4)		88.3			87.8

* Numbers are those of O(2) atoms.

** Error in parentheses is one standard deviation; for 87.6 (1) read $87.6 \pm 0.1^\circ$, etc.

the three magnesium atoms are actually very similarly coordinated. We are somewhat skeptical that the slight differences found here could lead to the two distinct doublets found in the Mössbauer spectrum of the orthorhombic form, and we suggest that the orthorhombic iron form studied by SCHMID and TROOSTER might have a structure slightly different from that of boracite. Actually the second doublet in the Mössbauer spectrum of the orthorhombic iron form is more nearly similar to the single doublet found in the *cubic* form than it is to the other doublet in the orthorhombic form. Conceivably the orthorhombic iron form could be related to orthorhombic boracite or to

the trigonal form by a type of "twinning" on the scale of a unit-cell or less. The boundary regions between "twins" might have cation coordination similar to that in the cubic form, accounting for the extra doublet.

Charge balance

On the basis of the simple ionic model developed by PAULING (1929), each tetrahedrally coordinated boron atom contributes 0.75 valence units (v.u.) to its associated oxygen atoms and each Mg or (Fe,Mg) cation contributes 0.40 v.u. to its associated oxygen atoms and the chlorine anion. These values sum to 2.25 v.u. for O(1), 1.90 v.u. for all O(2) atoms except those linking to B(3) of the triangle, which have the sum 2.15 v.u., and to 1.20 v.u. for the chlorine anion. The bond distances throughout most of the borate framework appear to be adjusted to reduce or augment these values appropriately for reaching the correct 2.00 or 1.00 sums. For example, in boracite the three oxygen atoms linking to B(3) have the longest B—O distances in their associated tetrahedra.

To take account of these changes in bond lengths, we use the empirical relationship between bond strengths and lengths proposed by ZACHARIASEN (1963). For all the O(2) atoms in boracite, the ZACHARIASEN bond strengths contributed by the boron atoms alone range from 1.55 to 1.69 v.u. Each O(2) atom is also coordinated to a magnesium atom, which is expected to contribute 0.40 v.u. by the PAULING model. A sum of less than 1.60 for the boron contributions to a particular O(2) atom is usually associated with a relatively short Mg—O bond, and a sum of greater than 1.60, with a longer Mg—O bond. Thus it appears that local charge balance is well maintained throughout most of the borate framework.

For the O(1) atom, however, which is coordinated by only three tetrahedral boron atoms, the sum of ZACHARIASEN bond strengths is only 1.68 v.u. The deficiency may be an indication that the structure tends to be electrostatically unstable in the vicinity of the O(1) atom, a reasonable assumption as it is here that the "ferro" shifts are partly localized. Another possibility for the deficiency is that the empirical relationship requires revision; further evidence is needed on this point. The bond strengths contributed in the PAULING model sum to 1.20 v.u. for the chlorine atom, but the Mg—Cl bonds are anomalously long. In the iron-rich trigonal form, the (Fe,Mg)—Cl bonds are not similarly

lengthened, possibly in accordance with the fact that this form is the lower temperature, and presumably more stable, of the three known forms: trigonal \rightarrow orthorhombic \rightarrow cubic.

Influence of cation and halogen radii on ferroelectric transition temperatures in boracite-like structures

A great many synthetic analogues of boracite have now been made, with various cations substituting for Mg and various halogens substituting for Cl. We find that the ferroelectric transition temperature of

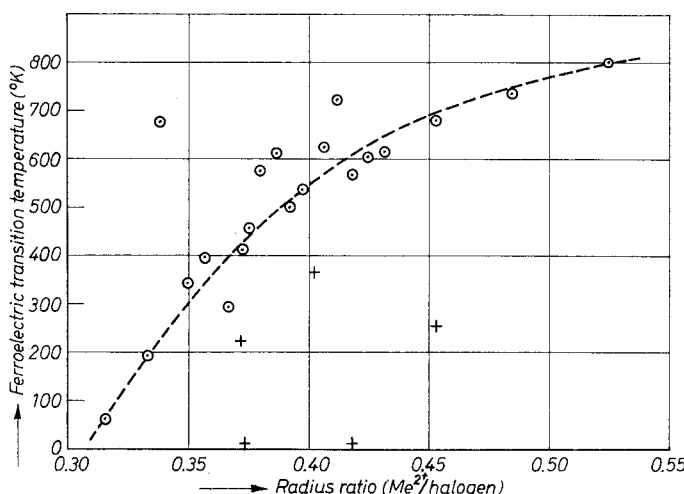


Fig. 4. Relation between cation/halogen radius ratio and ferroelectric transition temperature. Crosses represent compounds with Cu^{2+} or Cr^{2+} ; data from SCHMID (1965)

most of these compounds bears a systematic relation to the radius ratio of the cation and halogen ions, as shown in Fig. 4 (data from SCHMID, 1965). The transition temperature tends to increase with increasing radius of the cation and decreasing radius of the halogen ion. A number of points in Fig. 4 deviate greatly from the relation indicated by the line, but most of these represent compounds of two ions, Cu^{2+} and Cr^{2+} . These ions have the somewhat similar electronic configurations d^9 and d^4 , respectively, so that we may suspect some influence of bonding or crystal-field properties as a cause of the departure from the relationship, although the nature of such an influence is hard to specify.

Acknowledgements

We are indebted to J. S. HUEBNER, U. S. Geological Survey, for preparation of diffractometer patterns of the two compounds, and to R. C. ERD, U. S. Geological Survey, for supplying the crystals of the iron-rich analogue, which were originally given to him by R. KÜHN, Hannover, Germany.

References

- KEITSIRO AIZU (1968), Possible species of "ferroelastic" crystals and of simultaneously ferroelectric and ferroelastic crystals. *J. Physic. Soc. Japan* **27**, 387–396.
- LEROY E. ALEXANDER and GORDON S. SMITH (1964), Single-crystal diffractometry: The improvement of accuracy in intensity measurements. *Acta Crystallogr.* **17**, 1195–1201.
- DANIEL E. APPLEMAN, HOWARD T. EVANS, JR. and DAVID S. HANDWERKER (in press), Job 9214: Indexing and least-squares refinement of powder diffraction data. *U. S. Geol. Survey Computer Contrib.* No. 20. Nat. Tech. Info. Service, Springfield, Virginia 22151.
- E. ASCHER, H. RIEDER, H. SCHMID and H. STÖSSEL (1966), Some properties of ferromagnetoelectric nickel-iodine boracite, $\text{Ni}_3\text{B}_7\text{O}_{13}\text{I}$. *J. Appl. Physics* **37**, 1404–1405.
- P. J. BRAY, J. O. EDWARDS, J. G. O'KEEFE, V. F. ROSS and I. TATSUZAKI (1961), Nuclear magnetic resonance studies of B^{11} in crystalline borates. *J. Chem. Physics* **35**, 435–442.
- W. R. BUSING, K. O. MARTIN and M. A. LEVY (1962), ORFLS, a FORTRAN crystallographic least-squares program. *U.S. Oak Ridge Nat. Lab. Report ORNL-TM-305*.
- JOAN R. CLARK (1964), The crystal structure of tunellite, $\text{SrB}_6\text{O}_9(\text{OH})_2 \cdot 3\text{H}_2\text{O}$. *Amer. Mineral.* **49**, 1549–1568.
- ALESSANDRO CODA, GIUSEPPE GIUSEPPETTI and CARLA TADINI (1967), The crystal structure of wagnerite. *Accad. Naz. Lincei, Rend. Cl. Sci. fis., mat., natur.* **43**, 212–224.
- F. ALBERT COTTON and GEOFFREY WILKINSON (1966), *Advanced inorganic chemistry*, 2nd ed. Interscience, New York.
- DON T. CROMER and JOSEPH B. MANN (1968), X-ray scattering factors computed from numerical Hartree-Fock wave functions. *Acta Crystallogr. A* **24**, 321–324.
- DON T. CROMER and J. T. WABER (1965), Scattering factors computed from relativistic Dirac-Slater wave functions. *Acta Crystallogr.* **18**, 104–109.
- ALBERTO DAL NEGRO, CESARE SABELLI and LUCIANO UNGARETTI (1969), The crystal structure of macallisterite. *Accad. Naz. Lincei, Rend. Cl. Sci. fis., mat., natur.* **47**, 353–364.
- A. DAL NEGRO, L. UNGARETTI and C. SABELLI (1971), The crystal structure of aksaite. *Amer. Mineral.* **56**, 1553–1566.
- E. DORMANN (1970), Die optischen Absorptionsspektren von Ni^{2+} in Cl- und J-Boraziten. *J. Physics Chem. Solids* **31**, 199–214.

- ERIC DOWTY and JOAN R. CLARK (1972a), Borate framework of boracite and its relationship to the ferroelectric effects [abstr.]. Amer. Crystallogr. Assoc., Program and Abstracts, Albuquerque, New Mexico, p. 36.
- ERIC DOWTY and JOAN R. CLARK (1972b), Atomic displacements in ferroelectric trigonal and orthorhombic boracite structures. Solid State Commun. **10**, 543–548.
- V. DVORAK (1971), A thermodynamic theory of the cubic-orthorhombic phase transition in boracites. Czech. J. Physics **B21**, 1250–1261.
- S. G. FLEET and H. D. MEGAW (1962), The crystal structure of yoderite. Acta Crystallogr. **15**, 721–728.
- R. J. GILLESPIE (1963), The stereochemistry of five coordination. Part I. Non-transition elements. J. Chem. Soc. [London] **1963**, 4672–4678.
- F. HEIDE (1955), Über bemerkenswerte Borazitvorkommen in den Kalilagern des Südharzbezirkes. Chemie der Erde **17**, 211–216.
- T. ITO, N. MORIMOTO and R. SADANAGA (1951), The crystal structure of boracite. Acta Crystallogr. **4**, 310–316.
- CARROLL K. JOHNSON (1965), ORTEP, a FORTRAN thermal-ellipsoid plot program for crystal structure illustrations. ORNL-3794 (2nd rev., 1970). Clearinghouse for Federal Scientific and Technical Information, Springfield, Virginia 22151.
- J. KOBAYASHI, H. SCHMID and E. ASCHER (1968), Optical study on the ferroelectric orthorhombic phase of Fe-I-boracite. Physica Stat. Solidi **26**, 277–283.
- JUDITH A. KONNERT, JOAN R. CLARK and C. L. CHRIST (1970), Crystal structure of strontioginorite, $(\text{Sr,Ca})_2\text{B}_{14}\text{O}_{20}(\text{OH})_6 \cdot 5\text{H}_2\text{O}$. Amer. Mineral. **55**, 1911–1931.
- H. M. KRIZ and P. J. BRAY (1971), Doubts concerning the structure of boracites. J. Physics Chem. Solids **32**, 303–304.
- ROBERT KÜHN and INGEBURG SCHAACKE (1955), Vorkommen und Analyse der Boracit- und Ericaitkristalle aus dem Salzhorst von Wathlingen-Hanigsen. Kali und Steinsalz, No. 11, 33–42.
- LINUS PAULING (1929), The principles determining the structure of complex ionic crystals. J. Amer. Chem. Soc. **51**, 956–975.
- A. PERLOFF and S. BLOCK (1966), The crystal structure of the strontium and lead tetraborates, $\text{SrO} \cdot 2\text{B}_2\text{O}_3$ and $\text{PbO} \cdot 2\text{B}_2\text{O}_3$. Acta Crystallogr. **20**, 274–279.
- C. T. PREWITT and R. D. SHANNON (1968), Crystal structure of a high-pressure form of B_2O_3 . Acta Crystallogr. **B24**, 869–874.
- H. SCHMID (1965) Die Synthese von Boraziten mit Hilfe chemischer Transportreaktionen. J. Physics Chem. Solids **26**, 973–988.
- H. SCHMID (1970), Trigonal boracites—a new type of ferroelectric and ferromagnetoelectric that allows no 180° electric polarization reversal. Physica Stat. Solidi **37**, 209–223.
- H. SCHMID and J. M. TROOSTER (1967), Mössbauer effect and optical evidence for new phase transitions in Fe-Cl, Fe-Br, Fe-I, Co-Cl and Zn-Cl boracite. Solid State Commun. **5**, 31–35.
- R. D. SHANNON and C. T. PREWITT (1969), Effective ionic radii in oxides and fluorides. Acta Crystallogr. **B25**, 925–936.

- R. D. SHANNON and C. T. PREWITT (1970), Revised values of effective ionic radii. *Acta Crystallogr. B* **26**, 1046–1048.
- DONALD A. STEPHENSON and PAUL B. MOORE (1968), The crystal structure of grandidierite, $(\text{Mg}, \text{Fe})\text{Al}_3\text{SiBO}_9$. *Acta Crystallogr. B* **24**, 1518–1522.
- L. P. TORRE, S. C. ABRAHAMS, R. L. BARNS and K. NASSAU (1972), Ferroelastic reorientation and detwinning in synthetic boracite [abstr.]. Amer. Crystallogr. Assoc., Program and Abstracts, Albuquerque, New Mexico, p. 41.
- A. F. WELLS (1962), *Structural inorganic chemistry*, 3rd ed., Clarendon Press, Oxford, England.
- EMIL WENDLING, RENATE v. HODENBERG and ROBERT KÜHN (1972), Congolit, der trigonale Eisenboracit. *Kali und Steinsalz* **13**, 1–3.
- W. H. ZACHARIASEN (1963), The crystal structure of monoclinic metaboric acid. *Acta Crystallogr.* **16**, 385–392.
- A. ZIMMERMAN, W. BOLLMANN and H. SCHMID (1970), Observations of ferroelectric domains in boracites. *Physica Stat. Solidi (a)* **3**, 707–720.